Electronic Supplementary Information

A High-activity Cobalt-based MOF Catalyst for [2+2+2] Cycloaddition of Diynes and Alkynes: Insights on Alkyne Affinity and Selectivity Control

Fen Xu, Xiao-Ju Si, Xiao-Ning Wang, Hao-Dong Kou, Di-Ming Chen, Chun-Sen Liu* and Miao Du*

College of Material and Chemical Engineering, Zhengzhou University of Light Industry, Zhengzhou 450002, China

***** E-mail: chunsenliu@zzuli.edu.cn; dumiao@zzuli.edu.cn

RSC Advances

Contents

Section 1: General Materials and Methods S2

Section 2: Synthesis and Characterization for **Co-MOF-1** S3

Section 3: Single-Crystal X-Ray Crystallography S4~S6

Section 4: Additional Structural Figures for **Co-MOF-1** S7

Section 5: Gas Adsorption for **Co-MOF-1'** S8~S9

Section 6: General Procedure for [2+2+2] Cycloaddition S10

Section 7: Reusability of **Co-MOF-1'** S11

Section 8: Characterization of Diynes S12~S21

Section 9: Characterization of Products S22~S52

References S53

Section 1: General Materials and Methods

The HCPT ligand was prepared according to the literature method[S1] and all other chemicals for the synthesis of **Co-MOF-1** were obtained commercially. Concerning the procedure of [2+2+2] cycloaddition, all reactions and manipulations were carried out under the dry N_2 atmosphere or using standard Schlenk techniques. The anhydrous 1,2-dichloroethane (DCE) was distilled over CaH_2 before use and the diyne substrates were prepared according to the literature method,[S2~S6] whereas other reagents and solvents were obtained commercially and used as received. Column chromatography was performed on silica gel (300–400 mesh). Elemental analysis (C, H and N) was performed on a Vario EL III Elementar analyzer. IR spectrum was measured on a Bruker Tensor 27 OPUS FT-IR spectrometer with KBr pellet in 4000–400 cm^{-1} region. Thermogravimetric analysis (TGA) curves were recorded on a Perkin-Elmer Diamond SII thermal analyzer from room temperature to 800 ℃ with a heating rate of 10 ℃ min^{-1} under nitrogen atmosphere. Powder X-ray diffraction (PXRD) patterns were taken on a Rigaku (model Ultima IV) diffractometer, equipped with a Rigaku D/teX ultrahigh-speed position sensitive detector and Cu-Kα X-ray (40 kV and 40mA). The intensity data were collected in the step-scan mode with the scan rate of 2 °/min and step size of 0.02 °. Inductively coupled plasma mass spectroscopy (ICP-MS) analysis was conducted using a Perkin-Elmer ELAN 9000 instrument after degradation of the sample in HNO_3. Gas adsorption isotherms were taken on a Belsorp-Max automatic volumetric sorption apparatus under ultrahigh vacuum in a clean system. Ultrahigh-purity-grade N_2, C_2H_2, and He gases (> 99.999%) were used in all measurements. The experimental temperatures were maintained by temperature-programmed water bath (at 273 and 298 K) and liquid nitrogen (at 77 K). ^1H, ^{13}C and ^{19}F NMR were recorded on a 600 or 400 MHz Bruker NMR spectrometer in $CDCl_3$ using tetramethylsilane (TMS) as the internal standard. High resolution mass spectrometer (HRMS) data were obtained with Micromass HPLC-Q-TOF mass spectrometer.

Section 2: Synthesis and Characterization for **Co-MOF-1**

A mixture of $Co(NO_3)_2$ $6H_2O$ (0.044 g, 0.15 mmol) and HCPT (0.01 g, 0.05 mmol) was suspended in NMF (3 mL), H_2O (0.5 mL) and HBF_4 (3 drops, 37% aq), which was heated at 85 ℃ for 72 h under autogenous pressure in a Teflon-Bomb (23 mL). After cooling to room temperature, red polyhedral crystals were harvested by filtration, washed with NMF and MeOH in sequence, and dried in air. The yield was 70% for **Co-MOF-1** (based on HCPT). Elemental analysis calcd for **Co-MOF-1** ($C_{30}H_{43}Co_2N_{11}O_{15}$): C 39.35, H 4.73, N 16.83%; found: C 39.57, H 4.65, N 16.74%. IR (cm^{-1}): 3360 (br), 3098 (m), 1670 (s), 1603 (s), 1568 (s), 1415 (s), 1313 (m), 1250 (m), 1102 (m), 1057 (m), 863 (w), 840 (w), 782 (m).

Section 3: Single-Crystal X-Ray Crystallography

Crystal data for cycloadducts (**3ab**, **3ac**, **3ad**, **3af**, **3ag**, **3ah**, **3ba**, and **3ea**) were collected on a SuperNova diffractometer with Cu-Kα radiation (λ = 1.54178 Å) at 294(2) K. Multi-scan absorption corrections were taken with the *CrysAlisPro* program.[S7] Empirical absorption corrections were performed with spherical harmonics implemented in *SCALE3 ABSPACK* scaling algorithm. The structures were solved by direct methods and all non-H atoms were refined anisotropically by the full-matrix least-squares method with the SHELXTL crystallographic software package.[S8] All H atoms were located in calculated positions and treated in subsequent refinements as riding atoms. Crystallographic data and structural refinement details for the cycloadducts were summarized in Table S1 and Fig. S1.

Table S1. Crystallographic Data and Structure Refinement Details for Cycloadducts

	3ab	**3ac**	**3ad**	**3af**	**3ag**	**3ah**	**3ba**	**3ea**
Empirical formula	$C_{22}H_{21}NO_3S$	$C_{23}H_{23}NO_3S$	$C_{22}H_{21}NO_2S$	$C_{21}H_{18}ClNO_2S$	$C_{21}H_{18}FNO_2S$	$C_{21}H_{18}FNO_2S$	$C_{20}H_{16}ClNO_2S$	$C_{21}H_{17}NO$
Formula weight	379.46	393.48	363.46	383.87	367.42	367.42	369.85	299.36
Crystal system	monoclinic	orthorhombic	monoclinic	orthorhombic	monoclinic	monoclinic	triclinic	monoclinic
Space group	$P2_1$	$P2_12_12_1$	$P2_1$	$P2_12_12_1$	$P2_1/c$	$P2_1/c$	P-1	Pc
a / Å	7.9842(9)	8.4634(2)	7.9693(2)	7.0853(3)	20.5689(8)	19.4865(5)	7.5142(2)	15.5511(11)
b / Å	6.081(2)	9.3587(2)	6.1218(2)	9.0788(5)	10.9975(6)	6.17720(10)	12.7251(4)	7.0155(5)
c / Å	20.127(2)	25.6617(7)	19.3280(5)	29.0514(12)	7.9534(3)	15.7523(4)	18.0220(5)	7.3273(5)
α / °	90.00	90.00	90.00	90.00	90.00	90.00	88.481(2)	90.00
β / °	100.170(11)	90.00	101.204(2)	90.00	91.984(4)	109.925(3)	84.657(2)	94.253(6)
γ / °	90.00	90.00	90.00	90.00	90.00	90.00	89.958(2)	90.00
Volume / Å^3	961.9(4)	2032.57(9)	924.97(4)	1868.74(15)	1798.03(14)	1782.63(7)	1715.15(9)	797.20(10)
Z	2	4	2	4	4	4	4	2
D / g cm^{-3}	1.310	1.286	1.305	1.357	1.357	1.369	1.432	1.247
μ / mm^{-1}	1.673	1.601	1.674	2.973	1.813	1.828	3.218	0.596
F (000)	400.0	832.0	384.0	800.0	768.0	768.0	768.0	316.0
R_{int}	0.0458	0.0134	0.0323	0.0701	0.0250	0.0244	0.0330	0.0400
Goodness-of-fit on F^2	0.990	1.028	1.040	1.057	1.030	1.071	1.045	1.139
R_1 / wR_2 [$I>2\sigma(I)$]	0.0621/0.1625	0.0325/0.0859	0.0307/0.0818	0.0414/0.1070	0.0337/0.0923	0.0492/0.1395	0.0465/0.1196	0.0712/0.2176
R_1 / wR_2 (all data)	0.0813/0.1849	0.0349/0.0885	0.0345/0.0845	0.0603/0.1312	0.0345/0.0935	0.0542/0.1473	0.0506/0.1257	0.0737/0.2227
CCDC number	1491616	1491617	1491618	1491619	1491620	1491621	1491622	1491623

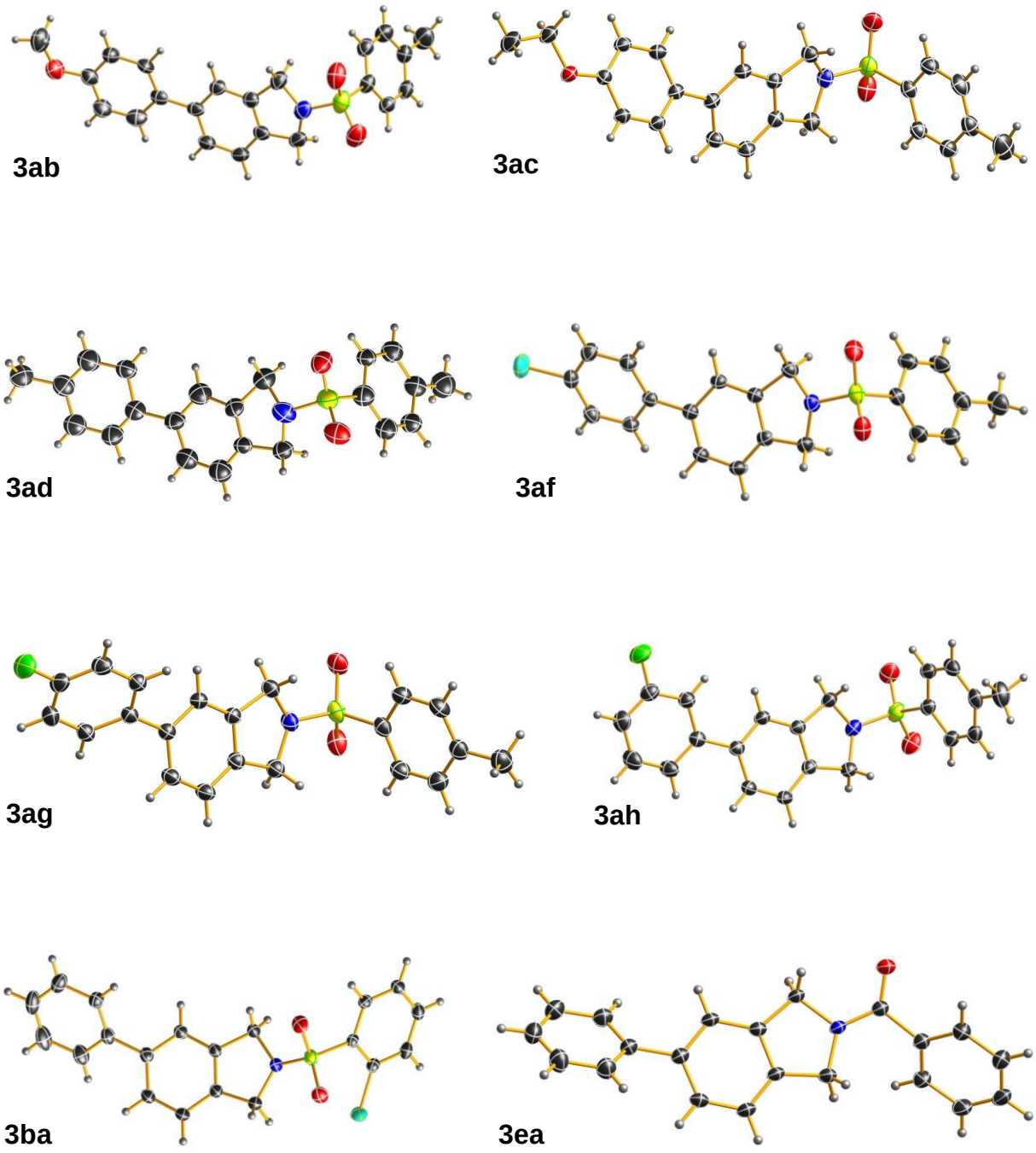

Figure S1. Crystal structures of **3ab**, **3ac**, **3ad**, **3af**, **3ag**, **3ah**, **3ba**, and **3ea** (C: black; H: gray; F: green; Cl: cyan; N: blue; O: red; S: yellow). The displacement ellipsoids are drawn at the 30% probability.

Section 4: Additional Structural Figures for **Co-MOF-1**

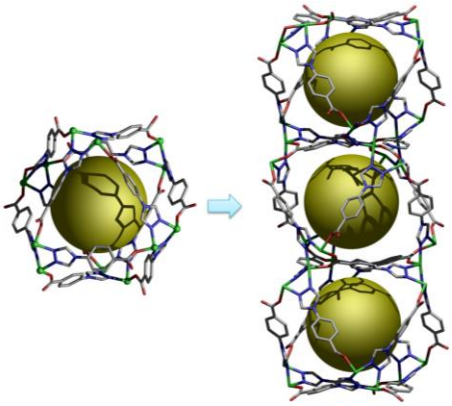

Figure S2. Serial octahedral cages in **Co-MOF-1** assembled *via* sharing the trigonal windows.

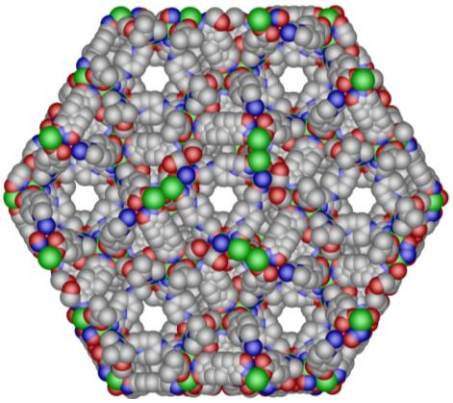

Figure S3. Spacing filling mode for the porous framework in **Co-MOF-1**.

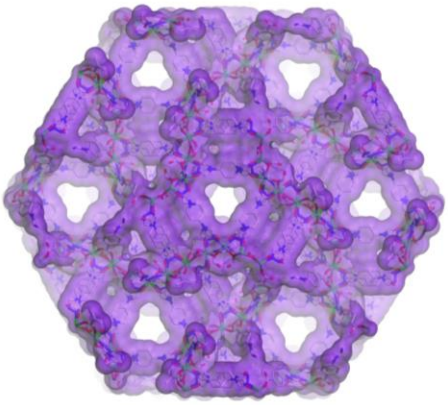

Figure S4. Connolly surface for the porous framework in **Co-MOF-1**.

Section 5: Gas Adsorption for **Co-MOF-1'**

Activation of Co-MOF-1. The as-synthesized **Co-MOF-1** (ca. 200 mg) was soaked in CH_2Cl_2 (50 mL) for 12 h and the extract was discarded. Fresh CH_2Cl_2 (50 mL) was subsequently added and the sample was allowed to soak for another 12 h. Such a refilling-and-removing cycle was repeated five times. After the removal of CH_2Cl_2 by decanting, the sample was transferred into a pre-weighed sample tube, evacuated (< 10^{-3} torr) at room temperature for 30 min, then dried using the outgas function of the adsorption instrument for 24 h at 70 ℃ before gas adsorption and desorption measurements.

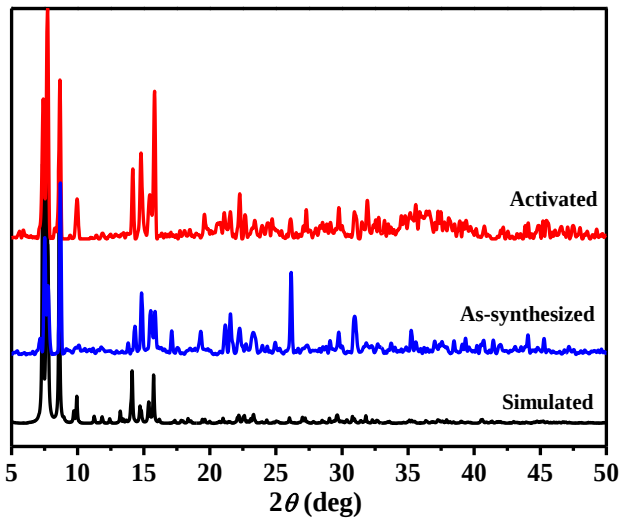

Figure S5. PXRD patterns for (black) simulated and (blue) as-synthesized **Co-MOF-1** as well as (red) the activated sample **Co-MOF-1'**.

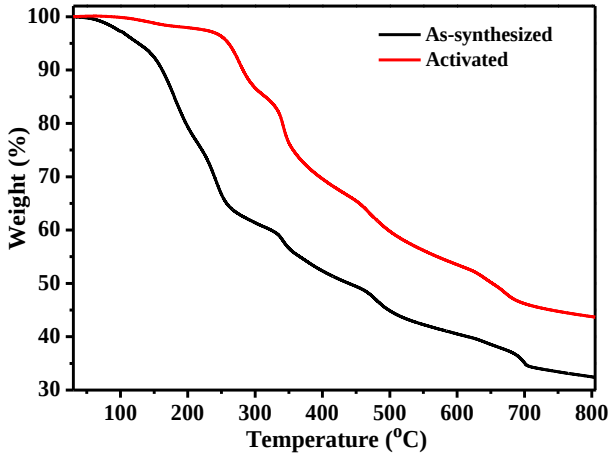

Figure S6. TGA curves for as-synthesized **Co-MOF-1** and activated **Co-MOF-1'**.

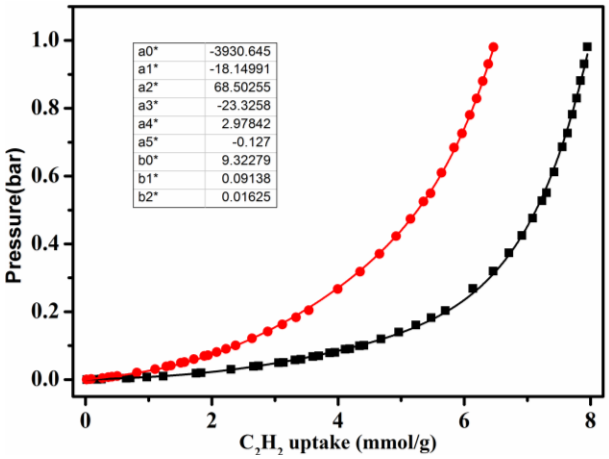

Figure S7. Virial fitting of the C_2H_2 adsorption isotherms for **Co-MOF-1'**.

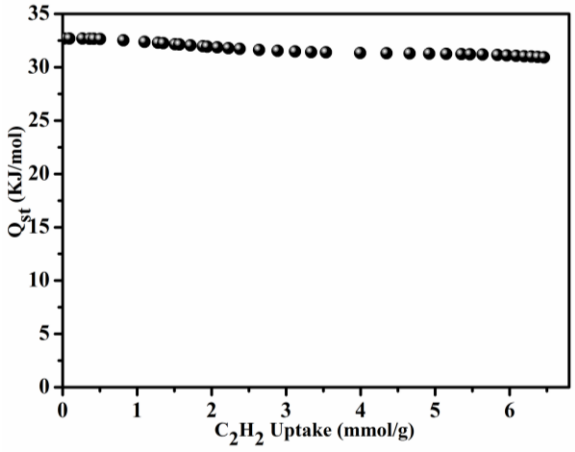

Figure S8. The calculated C_2H_2 adsorption enthalpies for **Co-MOF-1'**.

Section 6: General Procedure for [2+2+2] Cycloaddition

The activated **Co-MOF-1'** sample after gas adsorption tests was carefully treated by grind and then used in catalytic reactions. A mixture of **Co-MOF-1'** (10 mg), dppp (6.2 mg, 0.015 mmol), Zn powder and DCE (2 mL) was stirred at room temperature for 1 h, to which diyne and alkyne were added. The mixture was stirred at 80 °C for 24 h. After cooling to room temperature, DCE was evaporated and the oily residue was purified by column chromatography on silica gel with petroleum ether/ethyl acetate (polarity from 10:1 to 2:1).

Section 7: Reusability of **Co-MOF-1'**

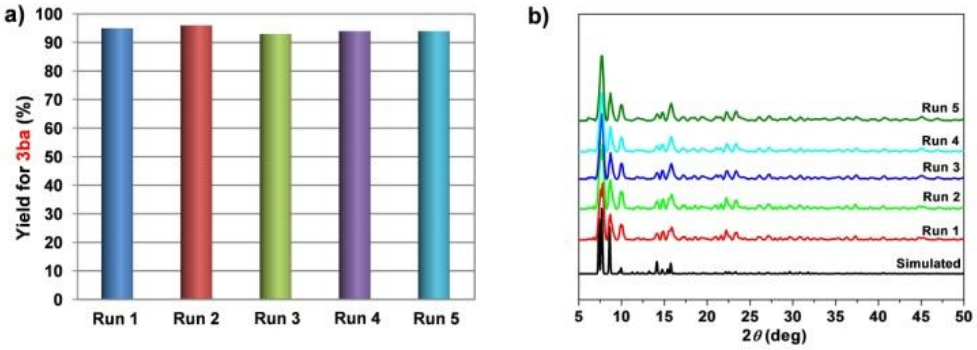

Figure S9 (a) Catalytic performance and reusability of Co-MOF-1' in [2+2+2] cycloaddition. (b) PXRD patterns for Co-MOF-1' catalyst after the reactions.

Section 8: Characterization of diynes

N,*N*-di(prop-2-yn-1-yl)benzenesulfonamide (1c)

White solid, eluent petroleum ether/ethyl acetate = 4:1. ^{1}H NMR (400 MHz, $CDCl_3$) δ 7.86 (d, *J* = 7.4 Hz, 2H), 7.57 (dt, *J* = 33.9, 7.4 Hz, 3H), 4.20 (d, *J* = 2.0 Hz, 4H), 2.16 (s, 2H). ^{13}C NMR (101 MHz, $CDCl_3$) δ 138.1, 133.2, 129.0, 127.8, 76.0, 74.1, 36.3.

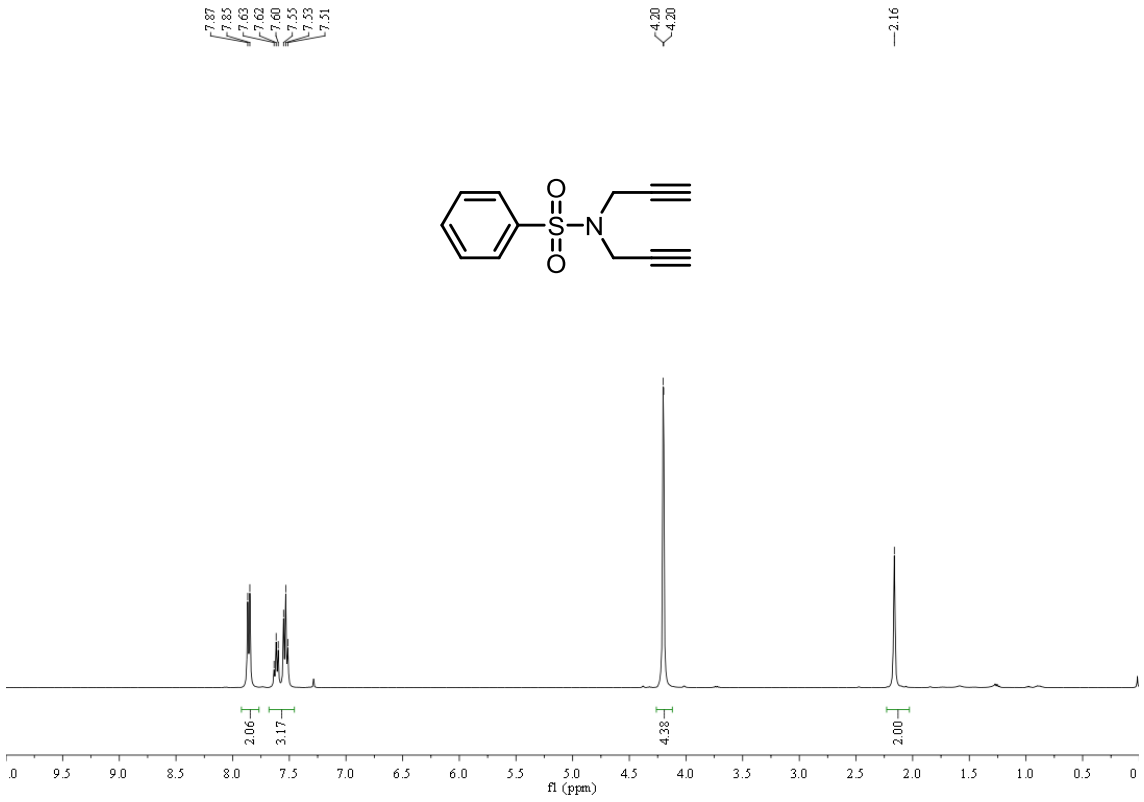

Figure S10. ^{1}H NMR (400 MHz, $CDCl_3$) of *N*,*N*-di(prop-2-yn-1-yl)benzenesulfonamide (**1c**).

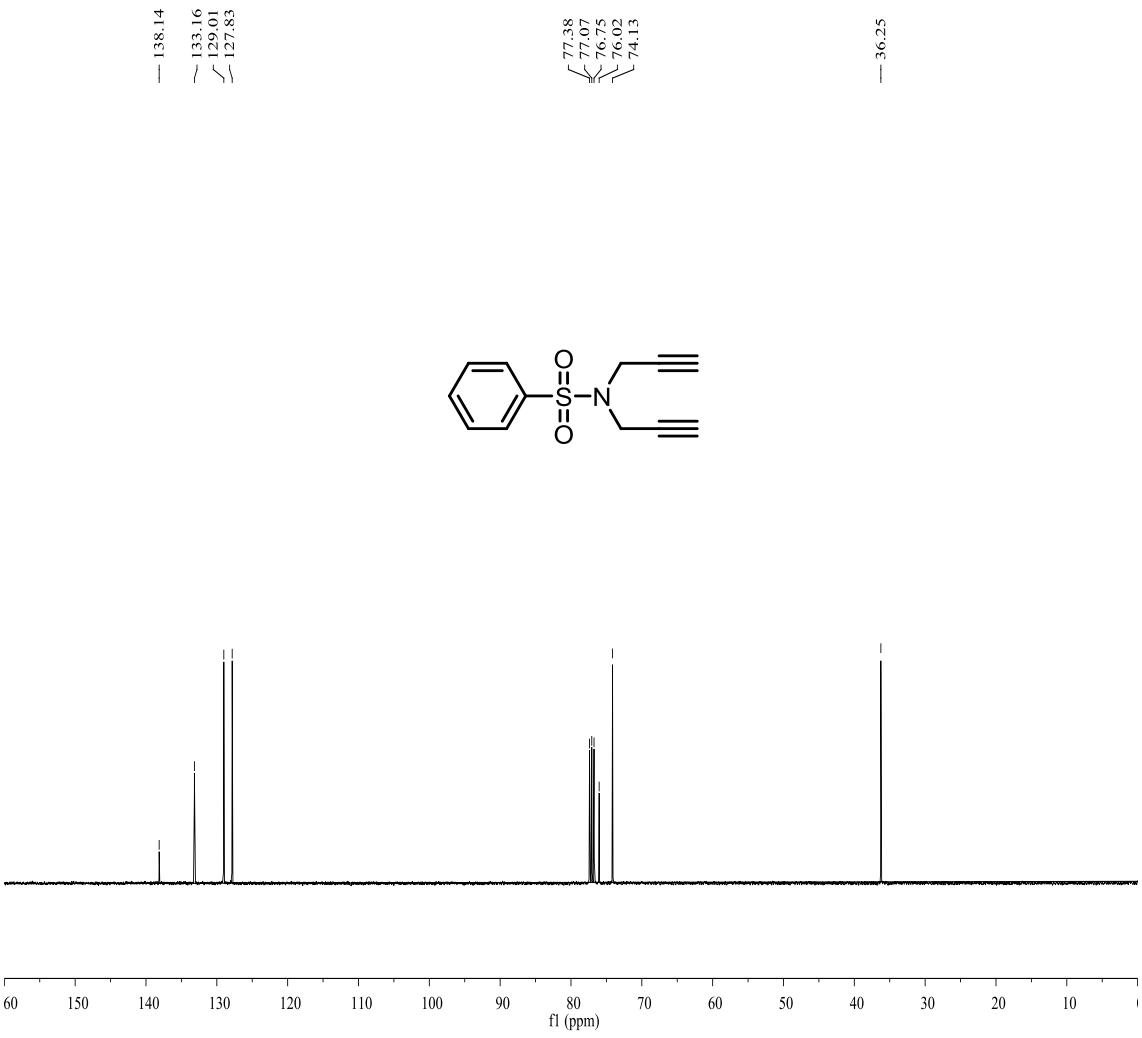

Figure S11. ^{13}C NMR (101 MHz, $CDCl_3$) of *N*,*N*-di(prop-2-yn-1-yl)benzenesulfonamide (**1c**).

2-fluoro-*N*,*N*-di(prop-2-yn-1-yl)benzenesulfonamide (1d)

White solid, eluent petroleum ether/ethyl acetate = 2:1. ^{1}H NMR (400 MHz, $CDCl_3$) δ 7.92 (t, *J* = 6.8 Hz, 1H), 7.70–7.52 (m, 1H), 7.29 (t, *J* = 7.6 Hz, 1H), 7.21 (t, *J* = 9.3 Hz, 1H), 4.30 (s, 4H), 2.17 (s, 2H). ^{13}C NMR (101 MHz, $CDCl_3$) δ 159.2 (d, *J* = 255.6 Hz), 135.4 (d, *J* = 8.6 Hz), 131.1, 127.0 (d, *J* = 14.2 Hz), 124.4 (d, *J* = 3.8 Hz), 117.1 (d, *J* = 21.7 Hz), 76.2, 73.7, 36.3, 36.2. ^{19}F NMR (376 MHz, $CDCl_3$) δ –107.66.

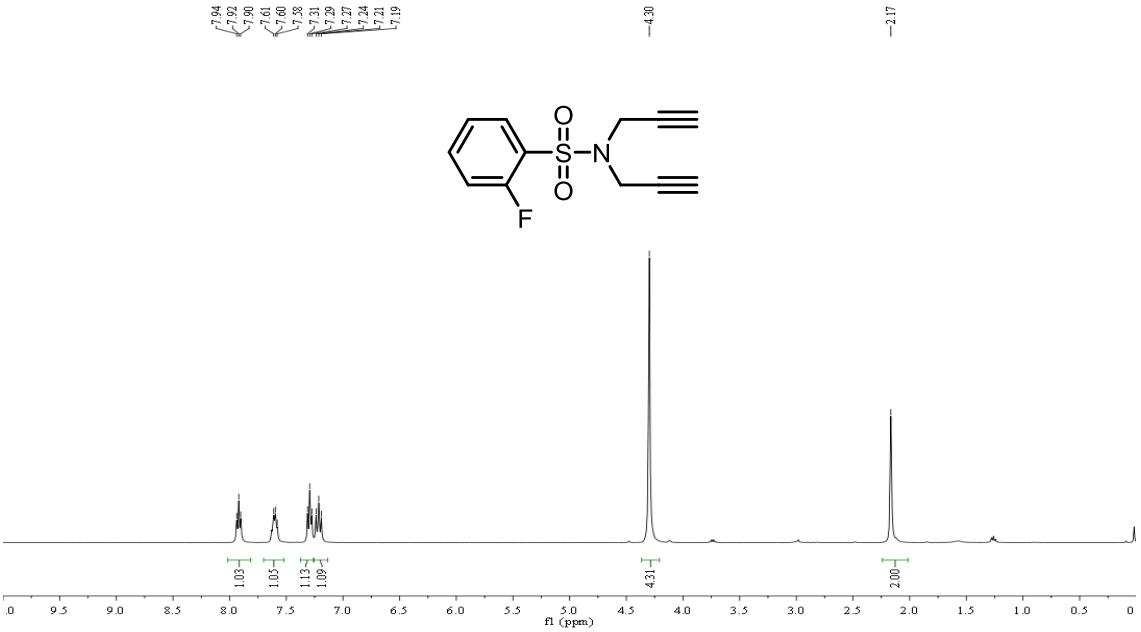

Figure S12. ^{1}H NMR (400 MHz, $CDCl_3$) of 2-fluoro-*N*,*N*-di(prop-2-yn-1-yl)benzenesulfonamide (**1d**).

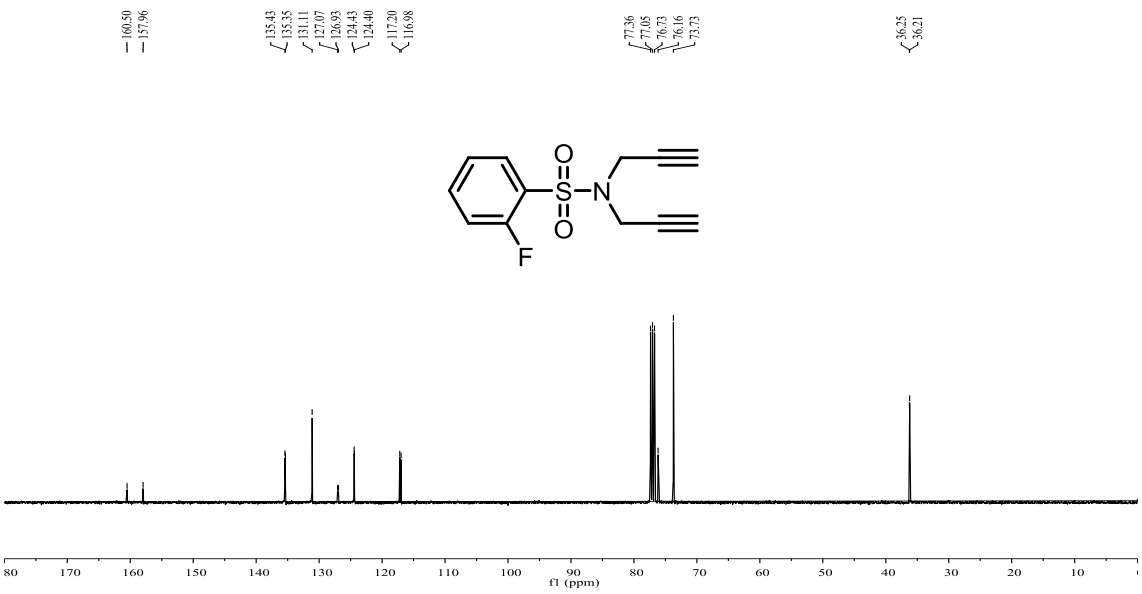

Figure S13. ^{13}C NMR (101 MHz, $CDCl_3$) of

2-fluoro-*N*,*N*-di(prop-2-yn-1-yl)benzenesulfonamide (**1d**).

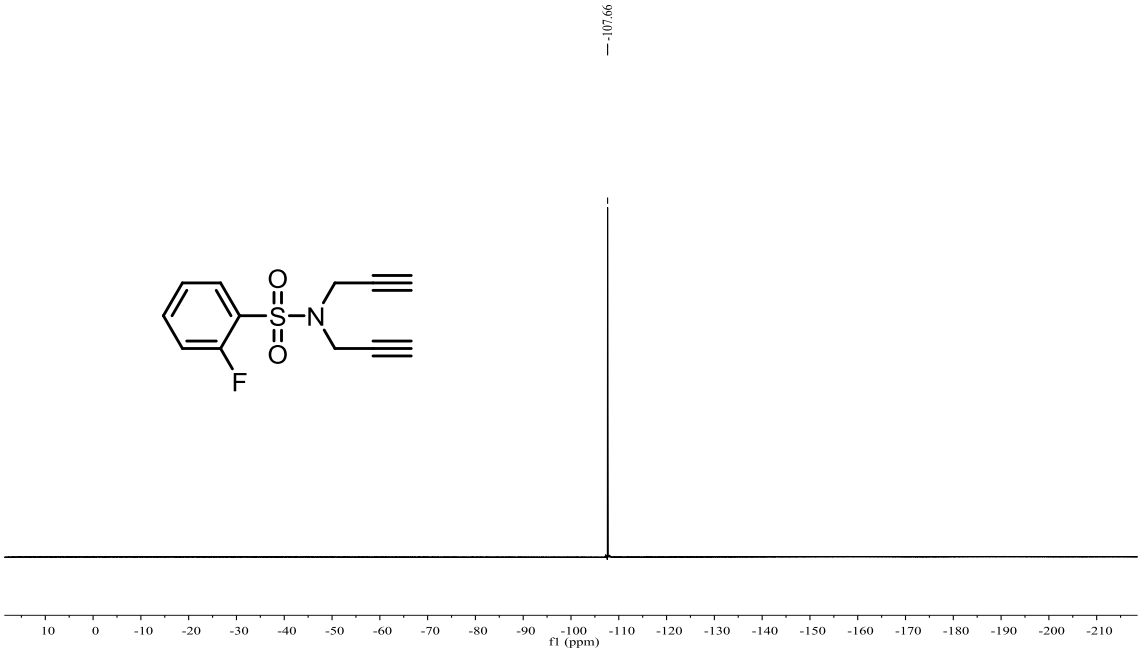

Figure S14. ^{19}F NMR (376 MHz, $CDCl_3$) of

2-fluoro-*N*,*N*-di(prop-2-yn-1-yl)benzenesulfonamide (**1d**).

_N_,_N_-di(prop-2-yn-1-yl)benzamide (1e)

White solid, eluent petroleum ether/ethyl acetate = 4:1. ^{1}H NMR (400 MHz, $CDCl_3$) δ 7.63–7.50 (m, 2H), 7.50–7.37 (m, 3H), 4.34 (m, 4H), 2.32 (s, 2H). ^{13}C NMR (101 MHz, $CDCl_3$) δ 170.8, 134.6, 130.5, 128.6, 127.2, 78.1, 72.8, 38.4, 33.8.

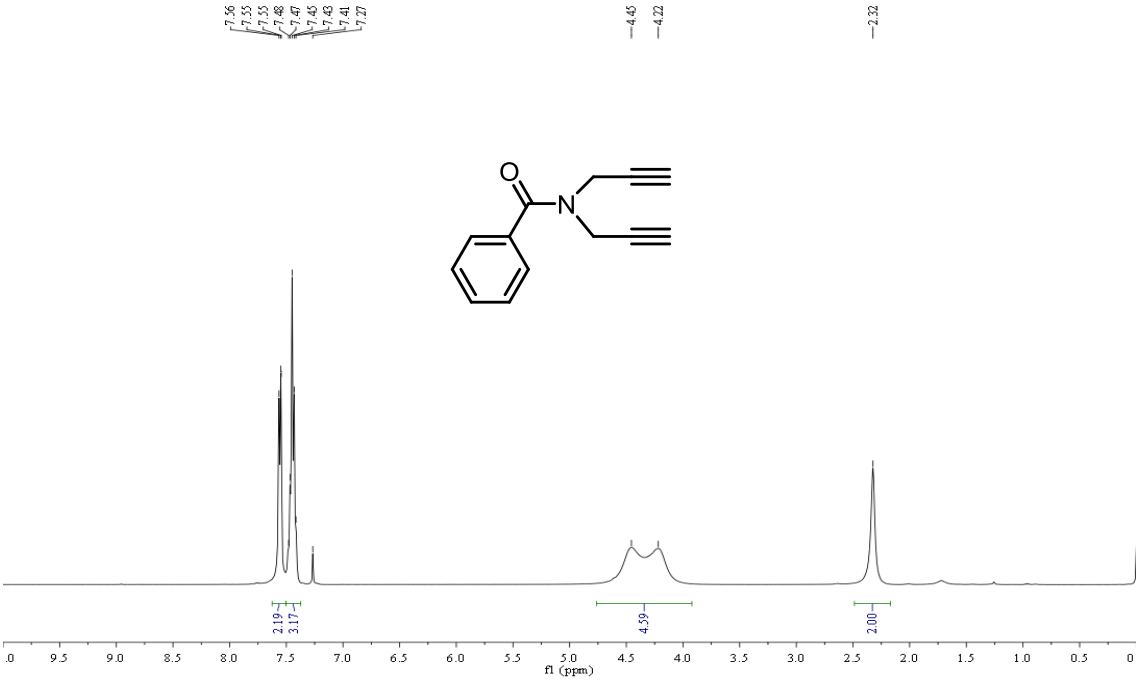

Figure S15. ^{1}H NMR (400 MHz, $CDCl_3$) of _N_,_N_-di(prop-2-yn-1-yl)benzamide (**1e**).

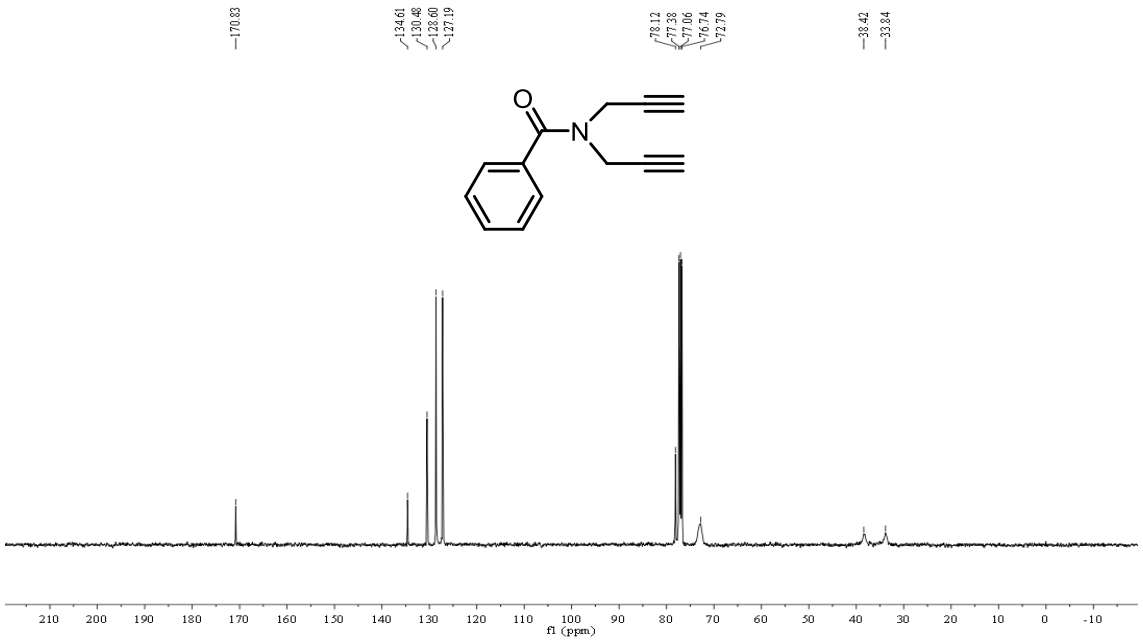

Figure S16. ^{13}C NMR (101 MHz, $CDCl_3$) of *N*,*N*-di(prop-2-yn-1-yl)benzamide (**1e**).

***N*-benzyl-*N*-(prop-2-yn-1-yl)prop-2-yn-1-amine (1f)**

White solid, eluent petroleum ether/ethyl acetate = 10:1. ^{1}H NMR (400 MHz, $CDCl_3$) δ 7.47–7.12 (m, 5H), 3.68 (s, 2H), 3.41 (d, *J* = 2.0 Hz, 4H), 2.26 (s, 2H). ^{13}C NMR (101 MHz, $CDCl_3$) δ 137.8, 129.3, 128.4, 127.5, 78.9, 73.3, 57.1, 41.9.

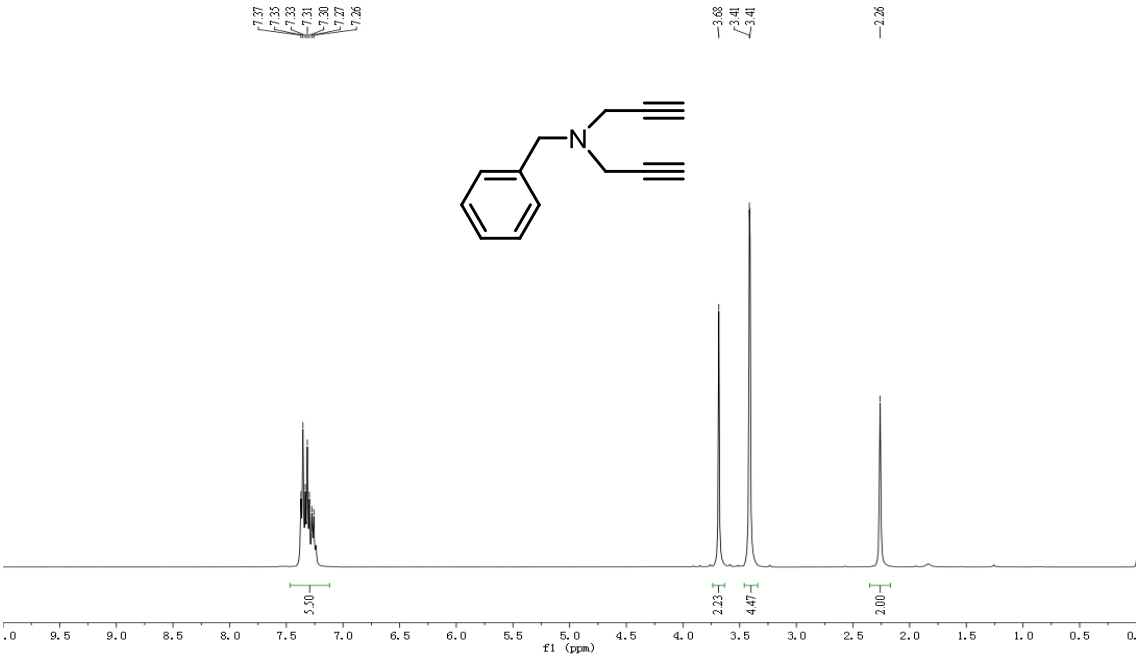

Figure S17. ^{1}H NMR (400 MHz, $CDCl_3$) of *N*-benzyl-*N*-(prop-2-yn-1-yl)prop-2-yn-1-amine (**1f**).

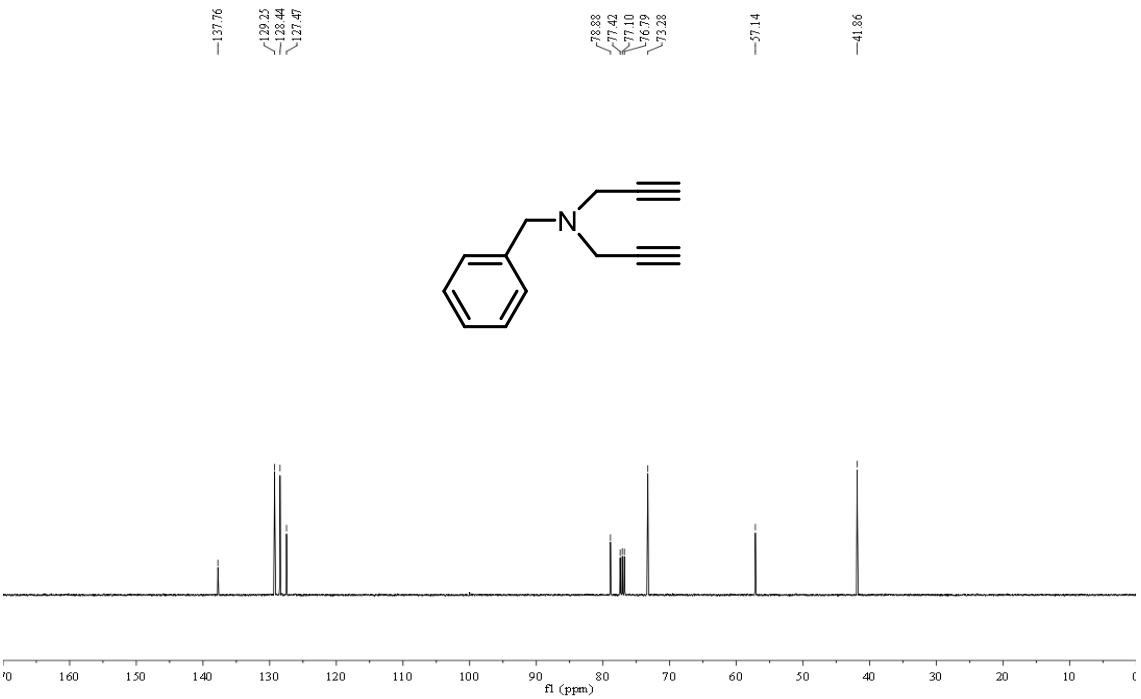

Figure S18. ^{13}C NMR (101 MHz, $CDCl_3$) of *N*-benzyl-*N*-(prop-2-yn-1-yl)prop-2-yn-1-amine (**1f**).

***N*,*N*-di(prop-2-yn-1-yl)methanesulfonamide (1g)**

White solid, eluent petroleum ether/ethyl acetate = 10:1. ^{1}H NMR (400 MHz, $CDCl_3$) δ 4.20 (d, *J* = 2.0 Hz, 4H), 2.99 (s, 3H), 2.42 (s, 2H). ^{13}C NMR (101 MHz, $CDCl_3$) δ 76.6, 74.6, 38.6, 36.5.

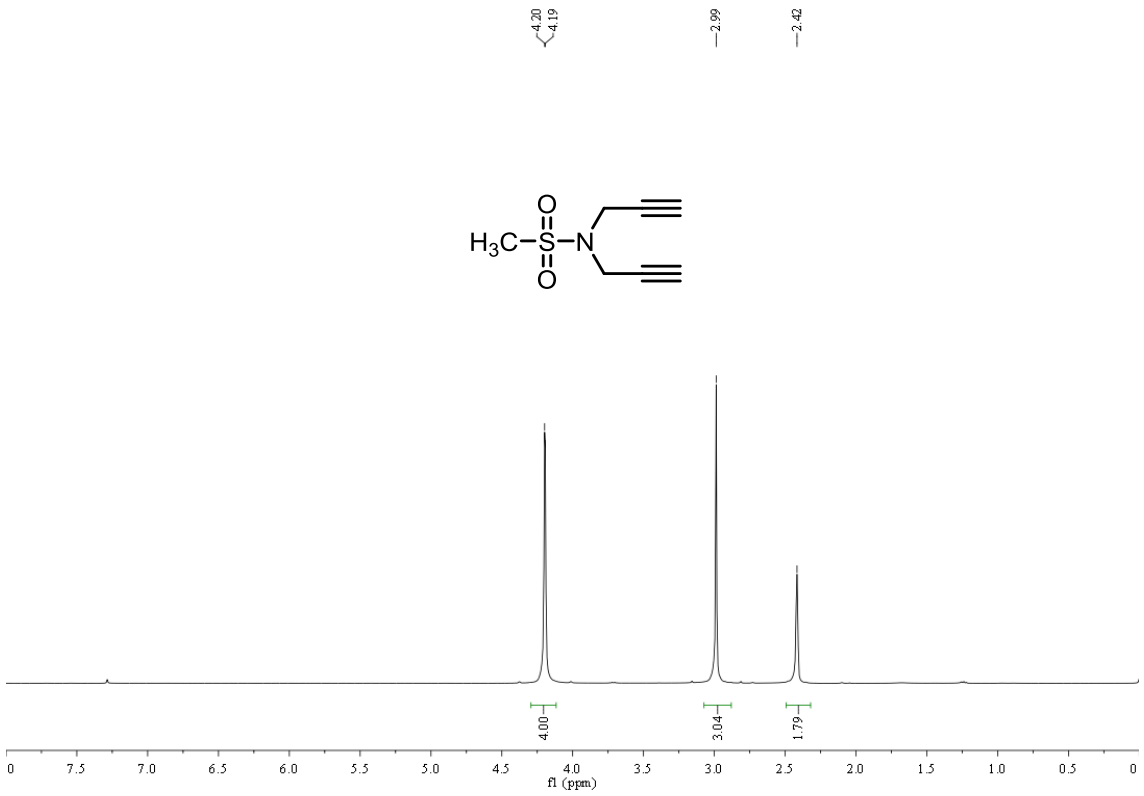

Figure S19. ^{1}H NMR (400 MHz, $CDCl_3$) of *N*,*N*-di(prop-2-yn-1-yl)methanesulfonamide (**1g**).

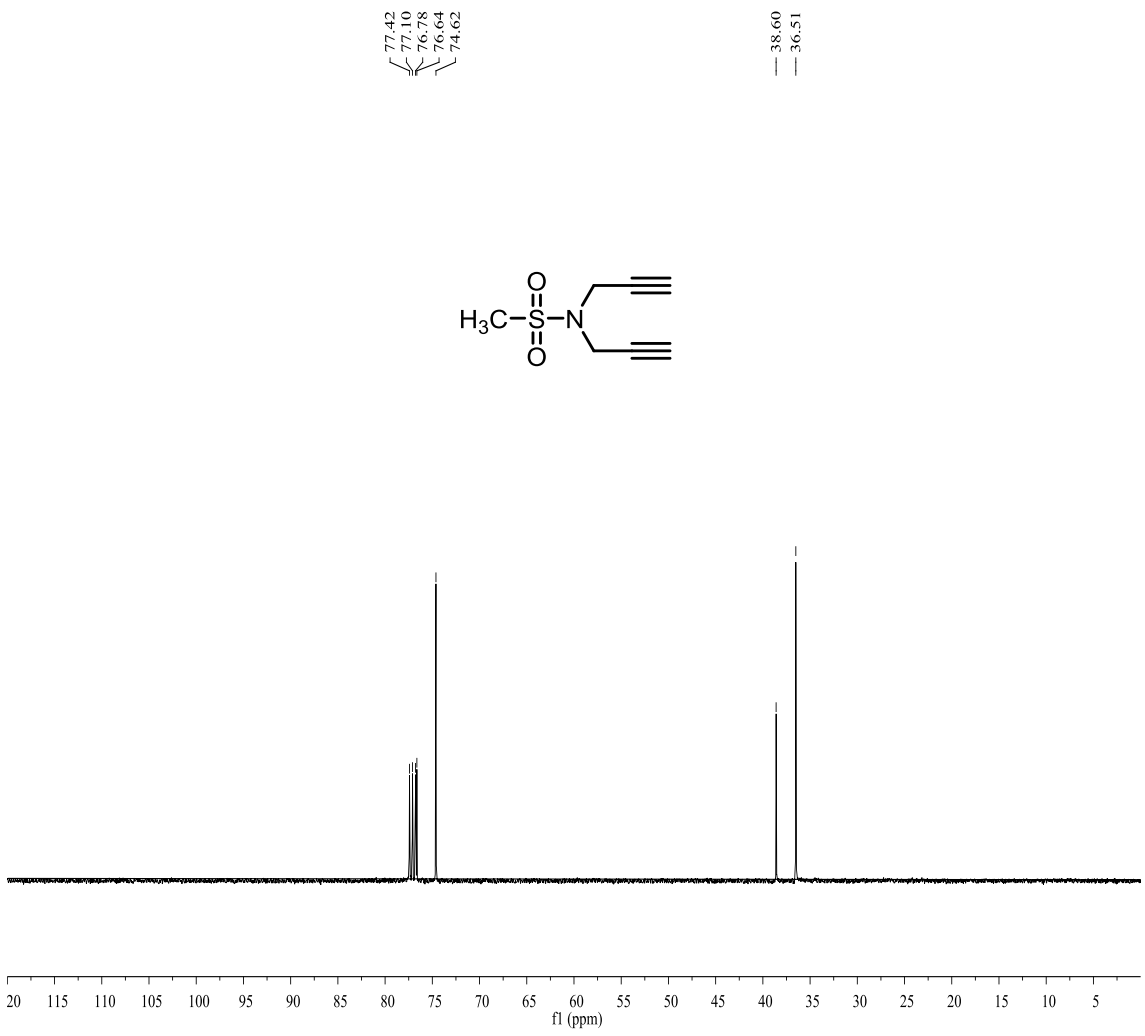

Figure S20. ^{13}C NMR (101 MHz, $CDCl_3$) of *N*,*N*-di(prop-2-yn-1-yl)methanesulfonamide (**1g**).

Section 9: Characterization of Products

5-phenyl-2-tosylisoindoline (3aa)

White solid (86% isolated yield), eluent petroleum ether/ethyl acetate = 4:1. ^{1}H NMR (600 MHz, $CDCl_3$) δ 7.79 (d, *J* = 8.3 Hz, 2H), 7.53–7.49 (m, 2H), 7.44 (m, 3H), 7.39–7.30 (m, 4H), 7.24 (d, *J* = 7.9 Hz, 1H), 4.67 (d, *J* = 7.3 Hz, 4H), 2.41 (s, 3H). ^{13}C NMR (151 MHz, $CDCl_3$) δ 143.7, 141.2, 140.5, 136.8, 135.1, 133.5, 129.8, 128.8, 127.6, 127.5, 127.1, 126.9, 122.9, 121.3, 53.7, 53.5, 21.5.

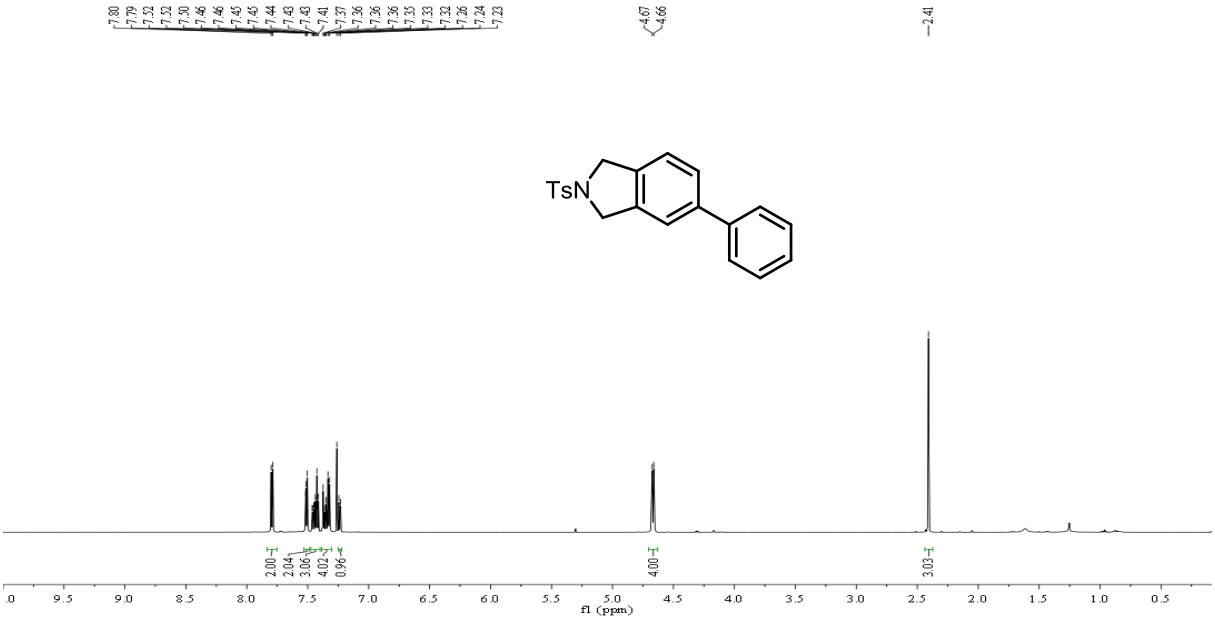

Figure S21. ^{1}H NMR (600 MHz, $CDCl_3$) of 5-phenyl-2-tosylisoindoline (**3aa**).

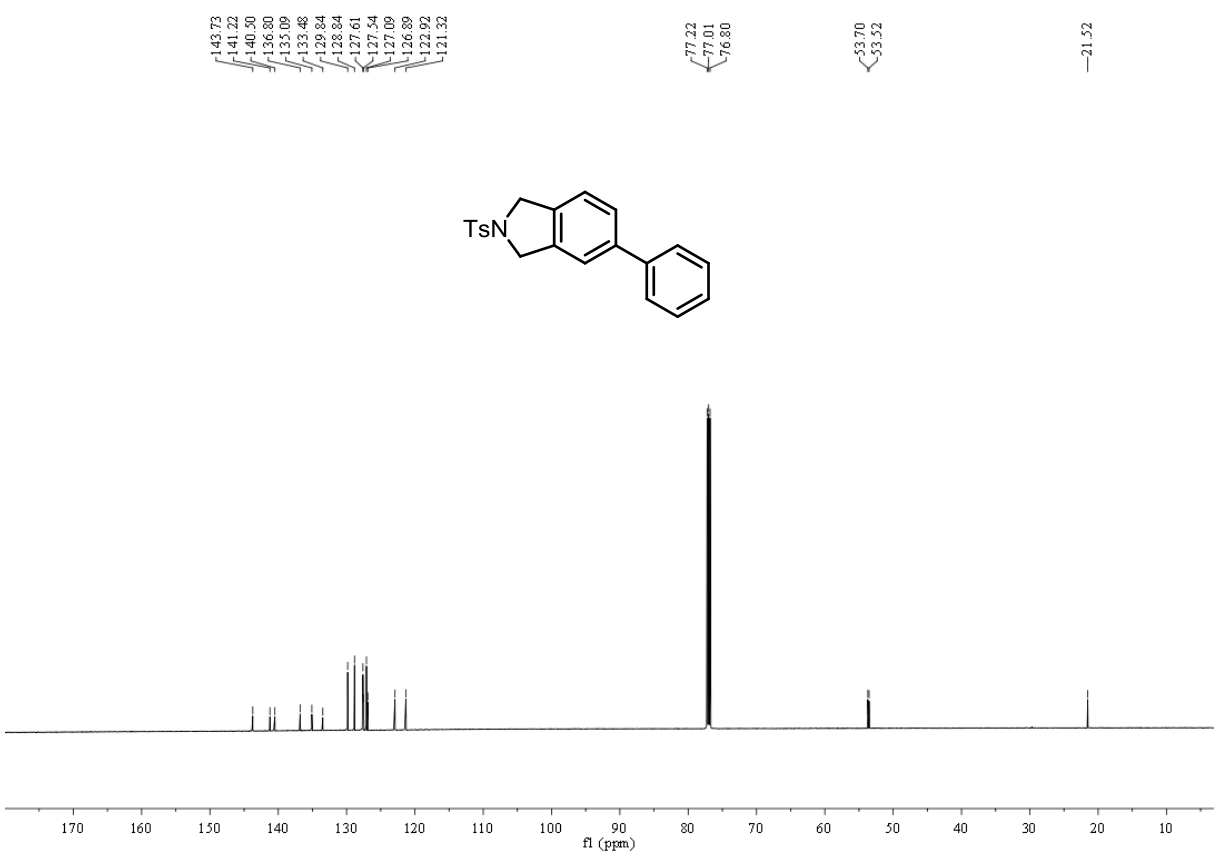

Figure S22. ^{13}C NMR (151 MHz, $CDCl_3$) of 5-phenyl-2-tosylisoindoline (**3aa**).

5-(4-methoxyphenyl)-2-tosylisoindoline (3ab)

White solid (87% isolated yield), eluent petroleum ether/ethyl acetate = 4:1. ^{1}H NMR (600 MHz, $CDCl_3$) δ 7.79 (d, *J* = 8.3 Hz, 2H), 7.47–7.42 (m, 2H), 7.41 (dd, *J* = 7.9, 1.4 Hz, 1H), 7.32 (d, *J* = 7.8 Hz, 3H), 7.21 (d, *J* = 8.0 Hz, 1H), 6.98–6.93 (m, 2H), 4.65 (d, *J* = 8.0 Hz, 4H), 3.84 (s, 3H), 2.40 (s, 3H). ^{13}C NMR (151 MHz, $CDCl_3$) δ 159.3, 143.7, 140.8, 136.7, 134.4, 133.5, 133.0, 129.8, 128.1, 127.6, 126.4, 122.9, 120.8, 114.2, 55.3, 53.7, 53.5, 21.5.

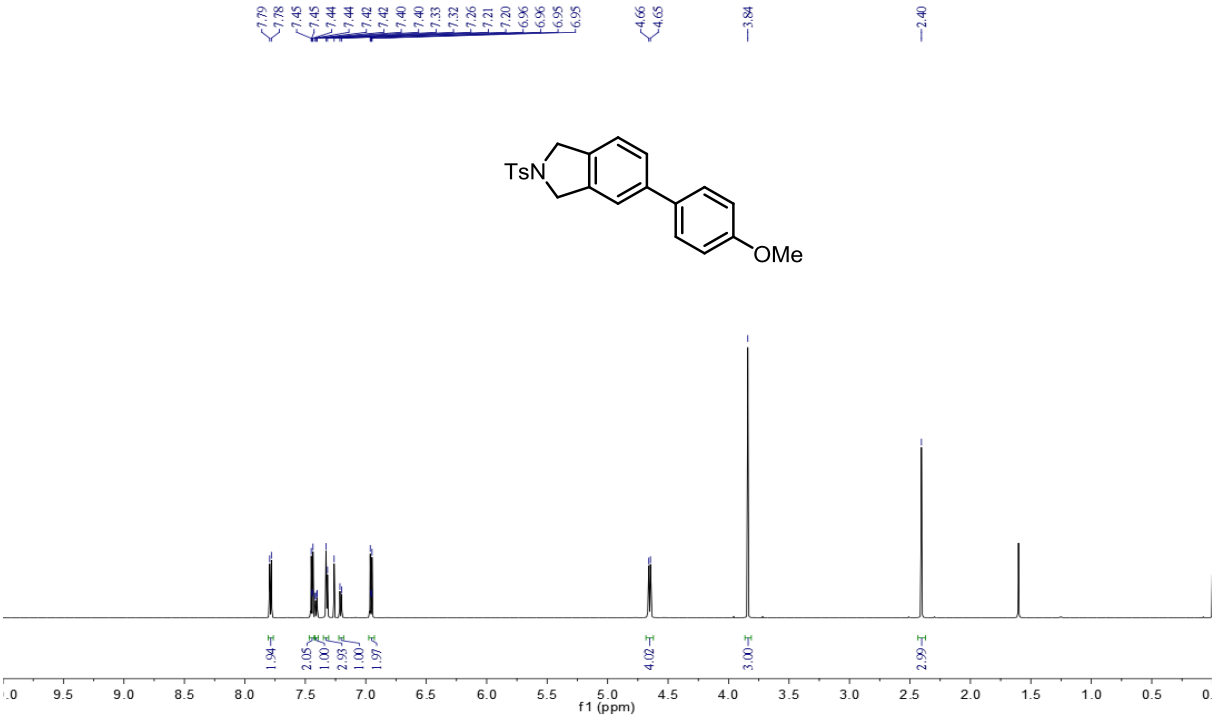

Figure S23. ^{1}H NMR (600 MHz, $CDCl_3$) of 5-(4-methoxyphenyl)-2-tosylisoindoline (**3ab**).

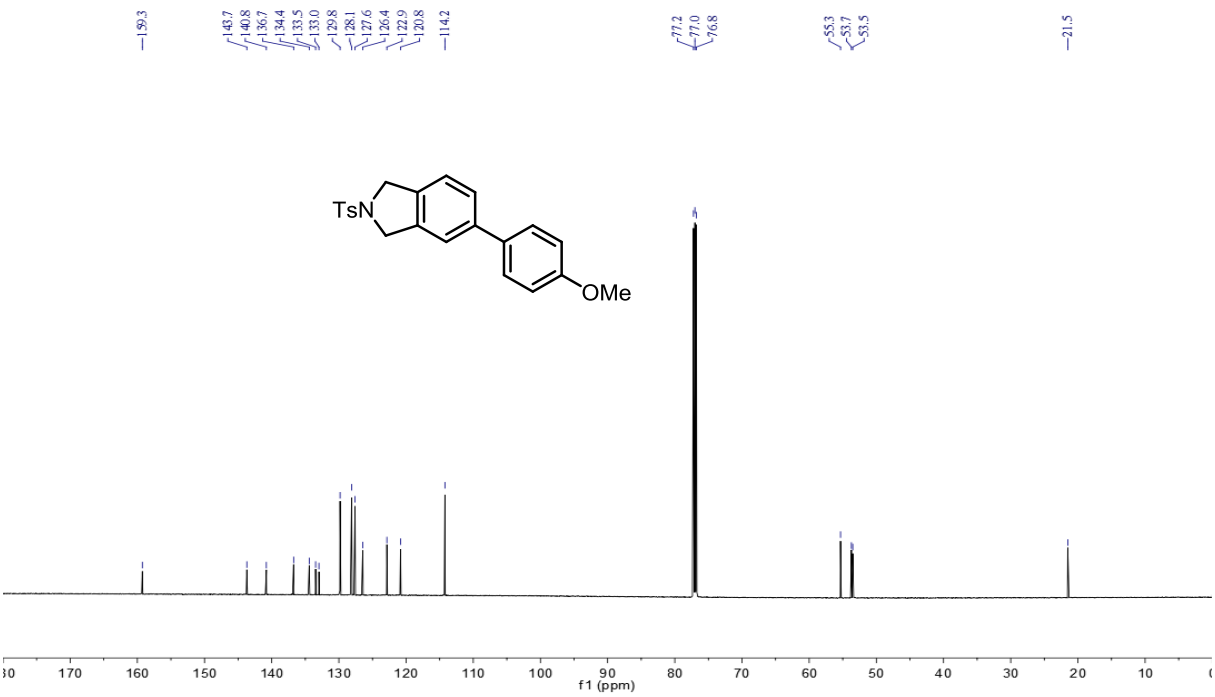

Figure S24. ^{13}C NMR (151 MHz, $CDCl_3$) of 5-(4-methoxyphenyl)-2-tosylisoindoline (**3ab**).

5-(4-ethoxyphenyl)-2-tosylisoindoline (3ac)

White solid (90% isolated yield), eluent petroleum ether/ethyl acetate = 4:1. ^{1}H NMR (600 MHz, $CDCl_3$) δ 7.79 (d, *J* = 8.3 Hz, 2H), 7.45–7.39 (m, 3H), 7.32 (d, *J* = 7.8 Hz, 3H), 7.20 (d, *J* = 8.0 Hz, 1H), 6.98–6.90 (m, 2H), 4.65 (d, *J* = 7.7 Hz, 4H), 4.06 (q, *J* = 7.0 Hz, 2H), 2.40 (s, 3H), 1.43 (t, *J* = 7.0 Hz, 3H). ^{13}C NMR (151 MHz, $CDCl_3$) δ 158.7, 143.7, 140.9, 136.7, 134.4, 133.5, 132.8, 129.8, 128.1, 127.6, 126.4, 122.8, 120.8, 114.7, 63.5, 53.7, 53.5, 21.5, 14.8.

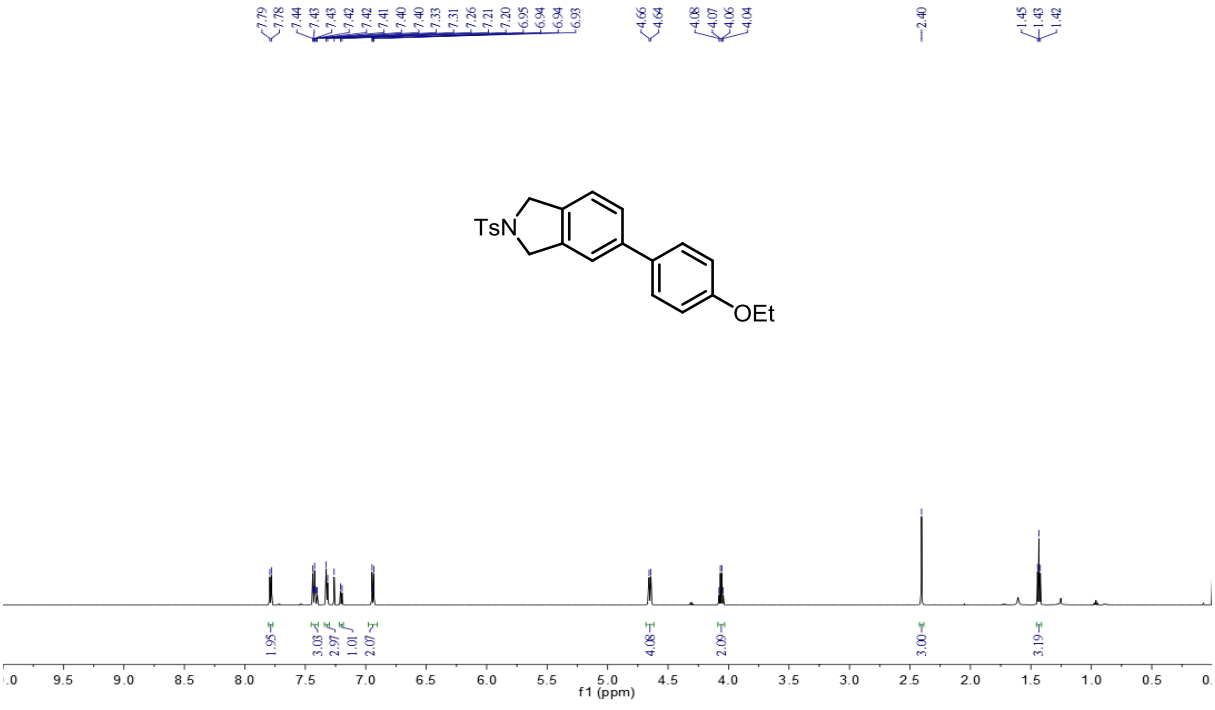

Figure S25. ^{1}H NMR (600 MHz, $CDCl_3$) of 5-(4-ethoxyphenyl)-2-tosylisoindoline (**3ac**).

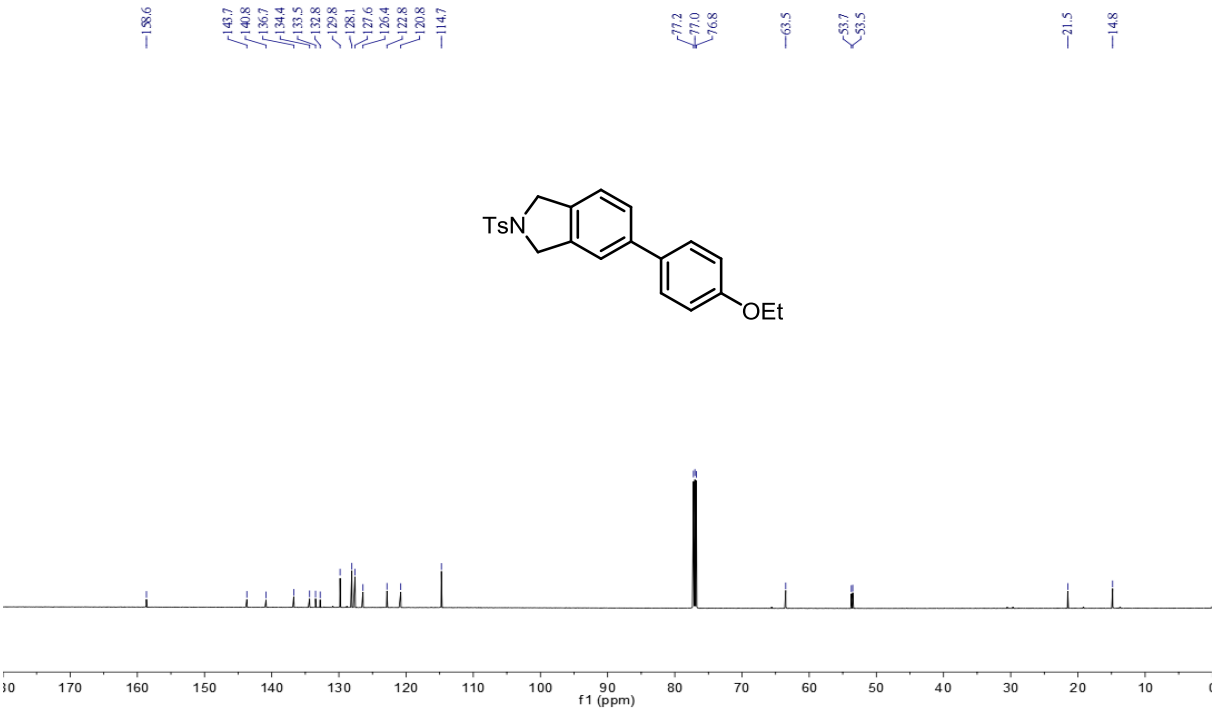

Figure S26. ^{13}C NMR (151 MHz, $CDCl_3$) of 5-(4-ethoxyphenyl)-2-tosylisoindoline (**3ac**).

5-(p-tolyl)-2-tosylisoindoline (3ad)

White solid (95% isolated yield), eluent petroleum ether/ethyl acetate = 4:1. ^{1}H NMR (600 MHz, $CDCl_3$) δ 7.79 (d, *J* = 8.2 Hz, 2H), 7.44 (d, *J* = 7.9 Hz, 1H), 7.41 (d, *J* = 8.1 Hz, 2H), 7.36 (s, 1H), 7.32 (d, *J* = 8.2 Hz, 2H), 7.23 (t, *J* = 8.0 Hz, 3H), 4.66 (s, 2H), 4.65 (s, 2H), 2.41 (s, 3H), 2.38 (s, 3H). ^{13}C NMR (151 MHz, $CDCl_3$) δ 143.7, 141.1, 137.6, 137.4, 136.7, 134.8, 133.5, 129.8, 129.6, 127.6, 126.9, 126.7, 122.9, 121.1, 53.7, 53.5, 21.5, 21.1.

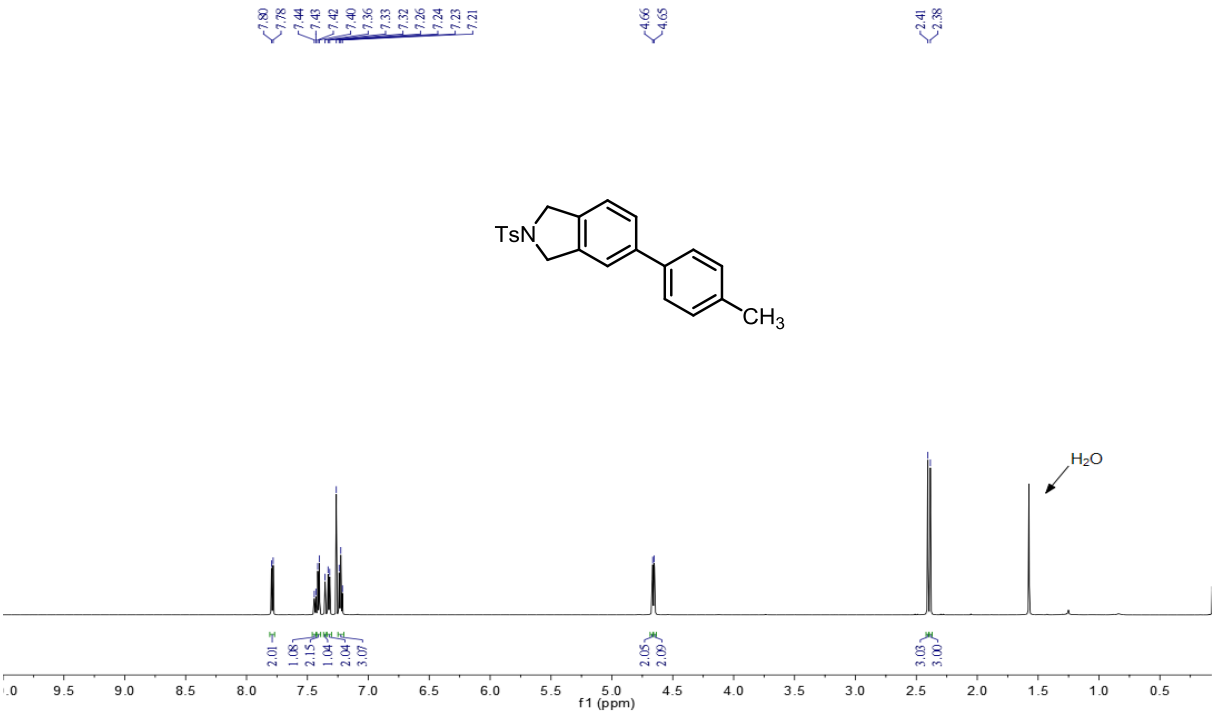

Figure S27. ^{1}H NMR (600 MHz, $CDCl_3$) of 5-(p-tolyl)-2-tosylisoindoline (**3ad**).

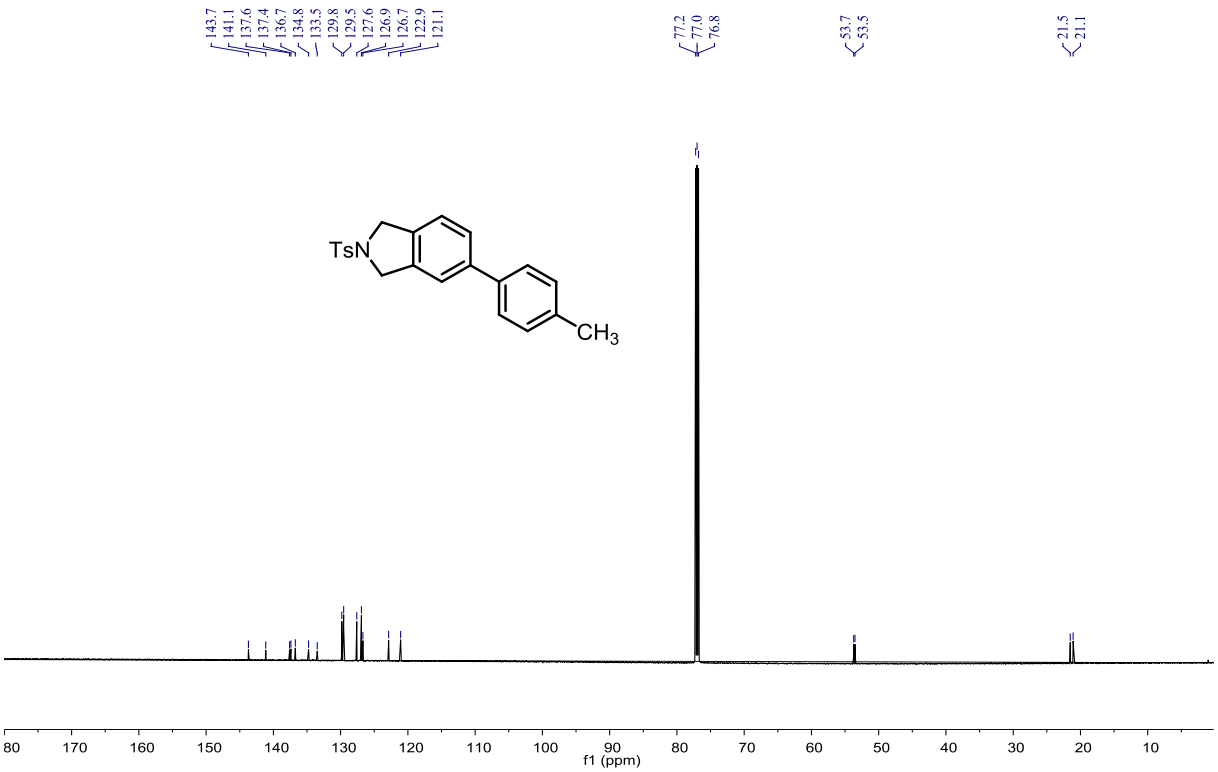

Figure S28. ^{13}C NMR (151 MHz, $CDCl_3$) of 5-(p-tolyl)-2-tosylisoindoline (**3ad**).

5-(4-chlorophenyl)-2-tosylisoindoline (3af)

White solid (88% isolated yield), eluent petroleum ether/ethyl acetate = 4:1. ^{1}H NMR (600 MHz, $CDCl_3$) δ 7.79 (d, *J* = 8.3 Hz, 2H), 7.45–7.37 (m, 5H), 7.33 (d, *J* = 8.1 Hz, 3H), 7.24 (d, *J* = 7.9 Hz, 1H), 4.66 (d, *J* = 6.5 Hz, 4H), 2.41 (s, 3H). ^{13}C NMR (151 MHz, $CDCl_3$) δ 143.8, 134.0, 138.9, 137.0, 135.5, 133.7, 133.5, 129.9, 129.0, 128.3, 127.6, 126.7, 123.1, 121.2, 53.7, 53.5, 21.5.

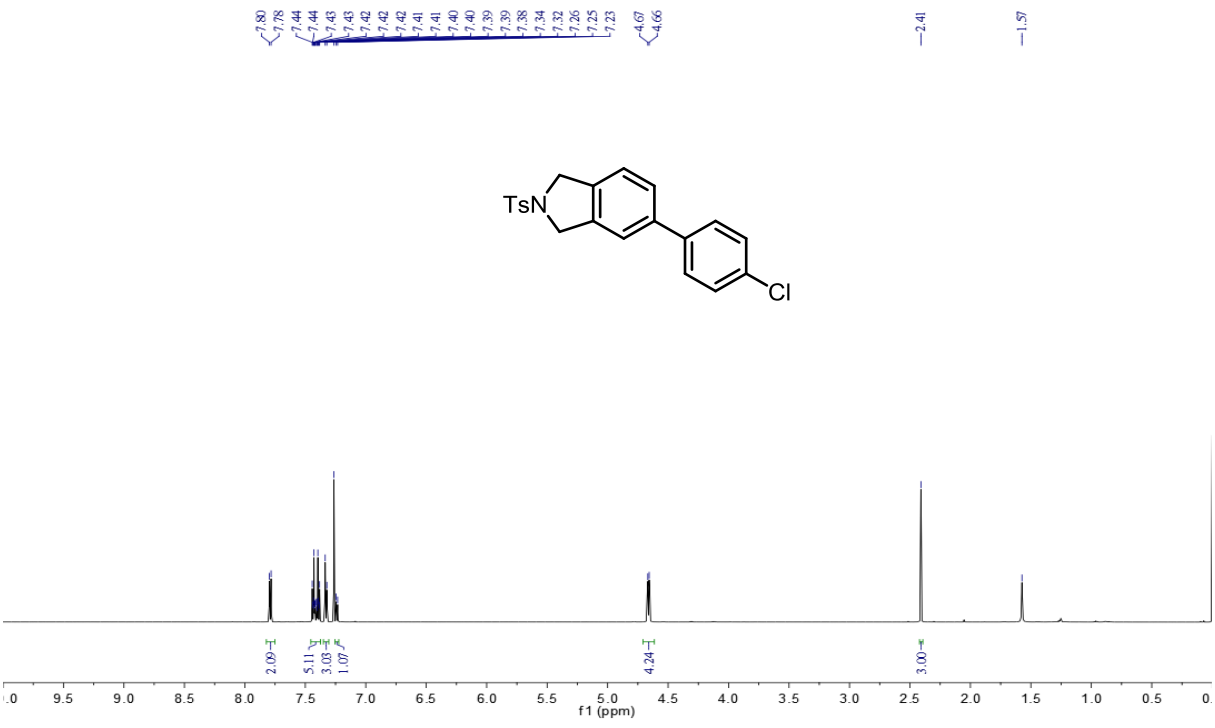

Figure S29. ^{1}H NMR (600 MHz, $CDCl_3$) of 5-(4-chlorophenyl)-2-tosylisoindoline (**3af**).

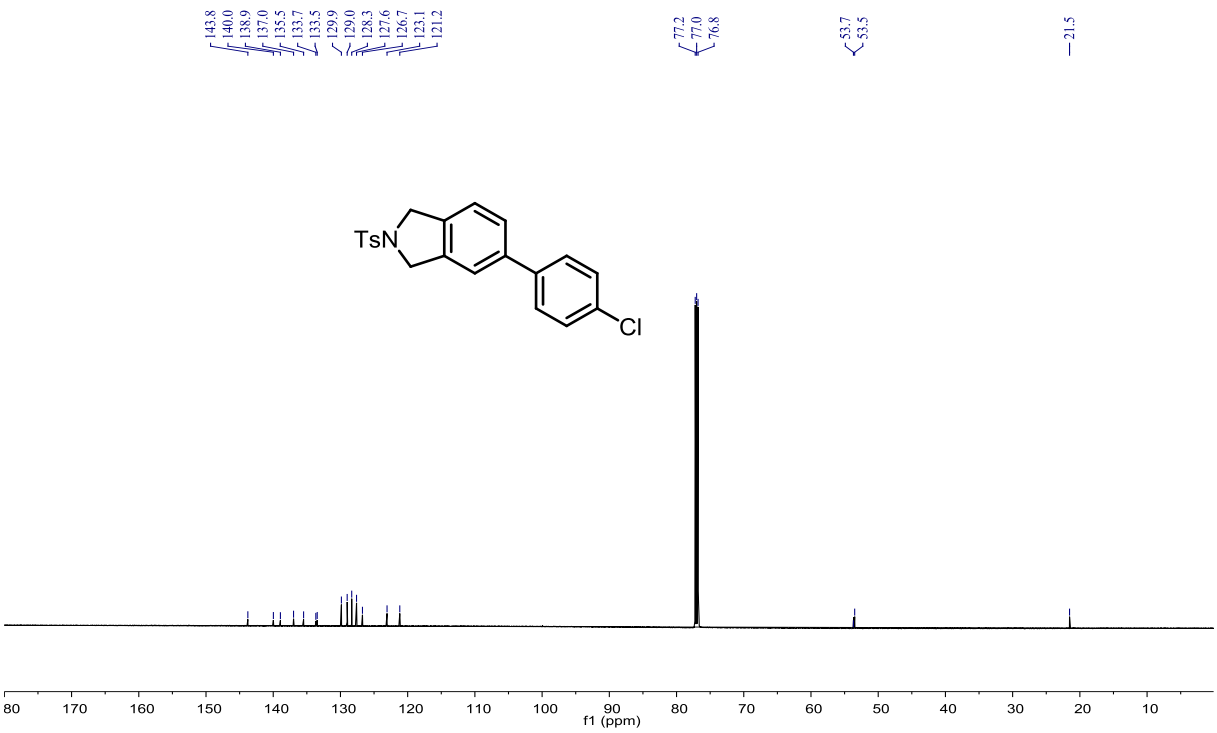

Figure S30. ^{13}C NMR (151 MHz, $CDCl_3$) of 5-(4-chlorophenyl)-2-tosylisoindoline (**3af**).

5-(4-fluorophenyl)-2-tosylisoindoline (3ag)

White solid (93% isolated yield), eluent petroleum ether/ethyl acetate = 2:1. ^{1}H NMR (600 MHz, $CDCl_3$) δ 7.79 (d, *J* = 8.3 Hz, 2H), 7.49–7.44 (m, 2H), 7.40 (dd, *J* = 7.9, 1.3 Hz, 1H), 7.33 (d, *J* = 8.0 Hz, 3H), 7.23 (d, *J* = 7.9 Hz, 1H), 7.11 (t, *J* = 8.7 Hz, 2H), 4.66 (d, *J* = 6.6 Hz, 4H), 2.41 (s, 3H). ^{13}C NMR (151 MHz, $CDCl_3$) δ 162.5 (d, *J* = 246.9 Hz), 143.8, 140.2, 137.0, 136.6 (d, *J* = 3.2 Hz), 135.1, 133.5, 129.9, 128.7 (d, *J* = 8.1 Hz), 127.6, 126.8, 123.0, 121.2, 115.7 (d, *J* = 21.5 Hz), 53.7, 53.5, 21.5. ^{19}F NMR (376 MHz, $CDCl_3$) δ –115.20.

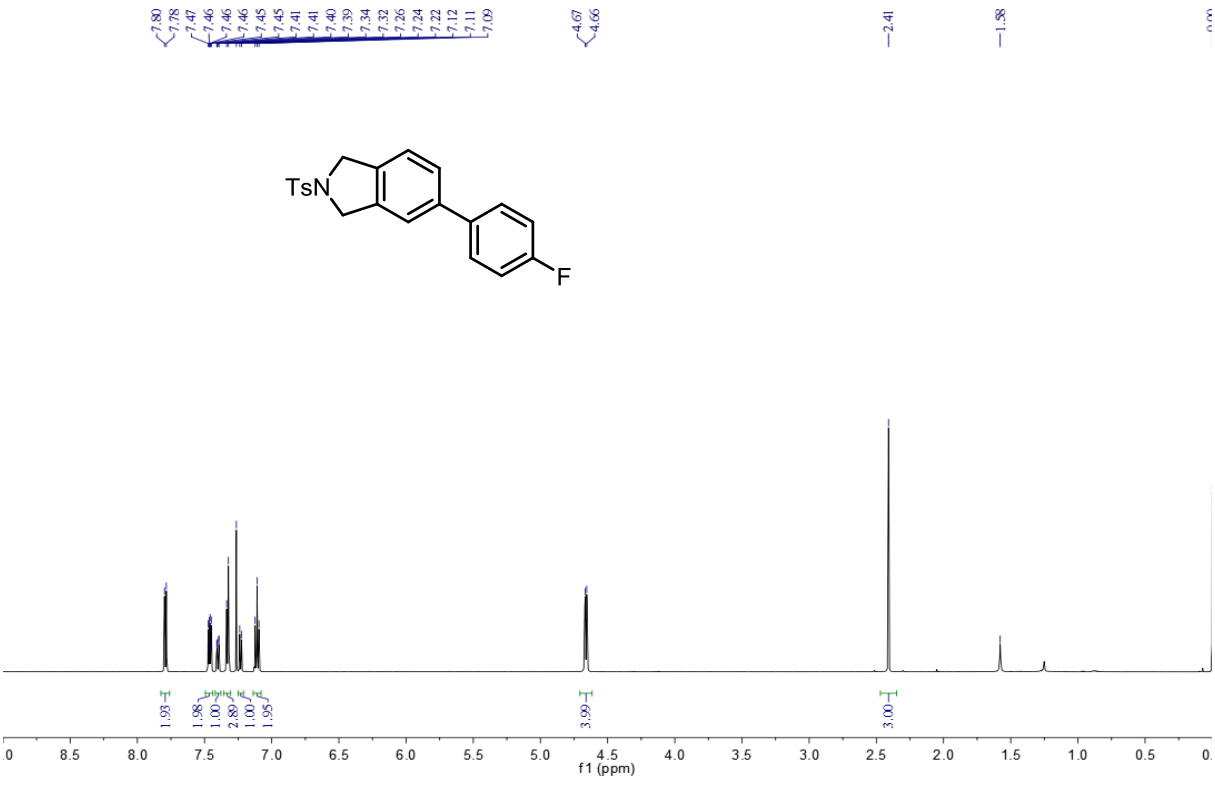

Figure S31. ^{1}H NMR (600 MHz, $CDCl_3$) of 5-(4-fluorophenyl)-2-tosylisoindoline (**3ag**).

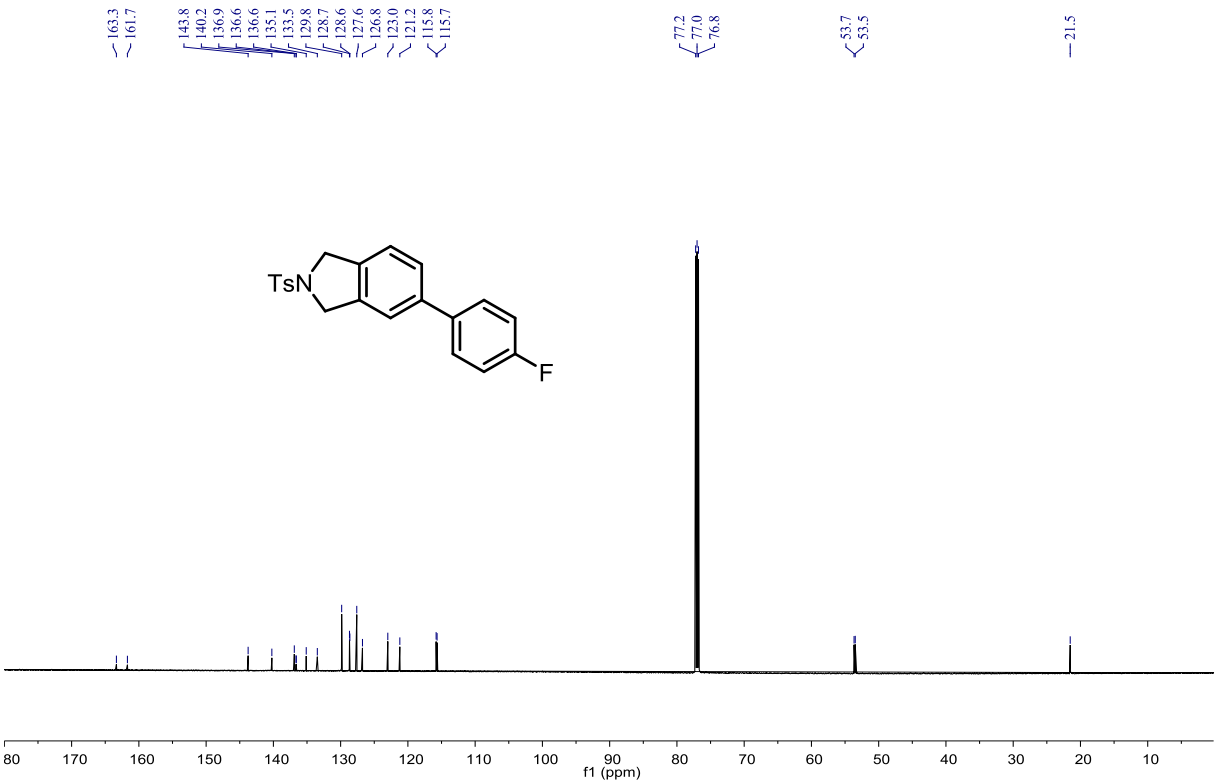

Figure S32. ^{13}C NMR (151 MHz, $CDCl_3$) of 5-(4-fluorophenyl)-2-tosylisoindoline (**3ag**).

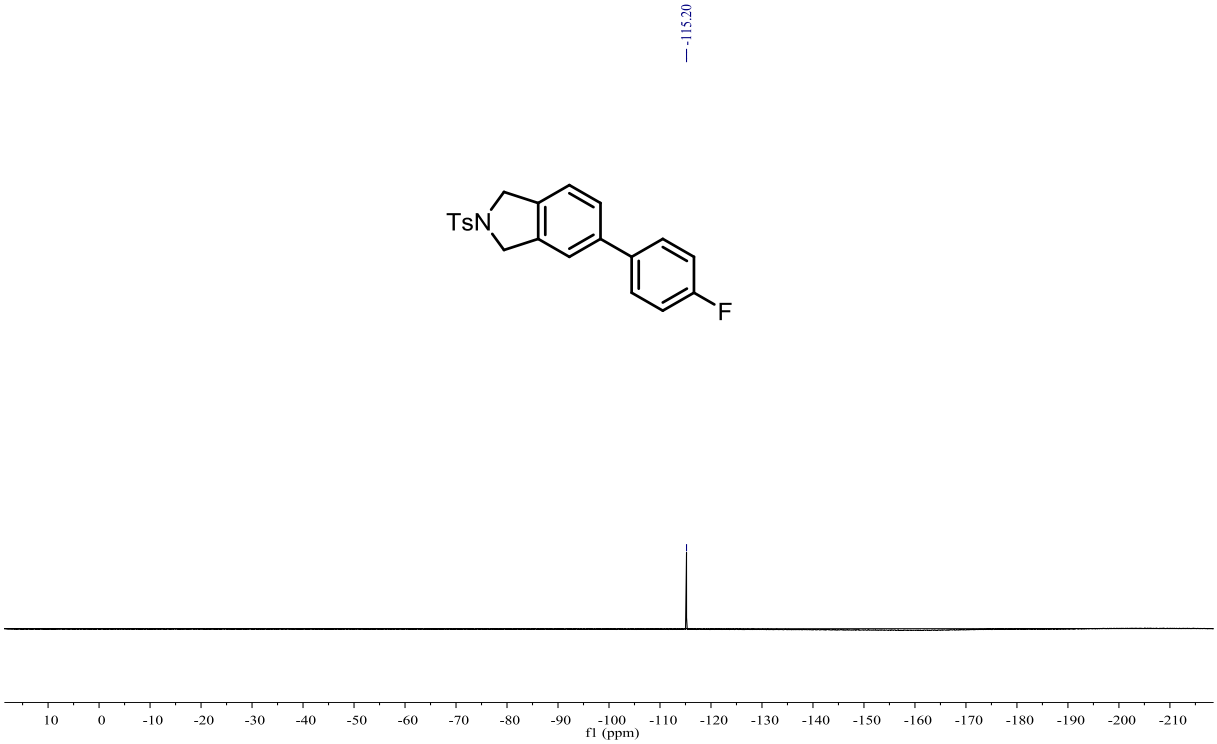

Figure S33. ^{19}F NMR (376 MHz, $CDCl_3$) of 5-(4-fluorophenyl)-2-tosylisoindoline (**3ag**).

5-(3-fluorophenyl)-2-tosylisoindoline (3ah)

White solid (86% isolated yield), eluent petroleum ether/ethyl acetate = 2:1. ^{1}H NMR (400 MHz, $CDCl_3$) δ 7.77 (d, *J* = 7.6 Hz, 2H), 7.47–7.12 (m, 8H), 7.01 (t, *J* = 7.9 Hz, 1H), 4.64 (s, 4H), 2.38 (s, 3H). ^{13}C NMR (101 MHz, $CDCl_3$) δ 163.2 (d, *J* = 246.1 Hz), 143.8, 142.9, 142.8, 140.0, 137.0, 135.8, 133.7, 130.4 (d, *J* = 8.4 Hz), 129.9, 127.6, 126.9, 123.10, 122.8 (d, *J* = 2.7 Hz), 121.3, 114.2 (dd, *J* = 34.7, 21.7 Hz), 53.7, 53.5, 21.5. ^{19}F NMR (376 MHz, $CDCl_3$) δ –112.82.

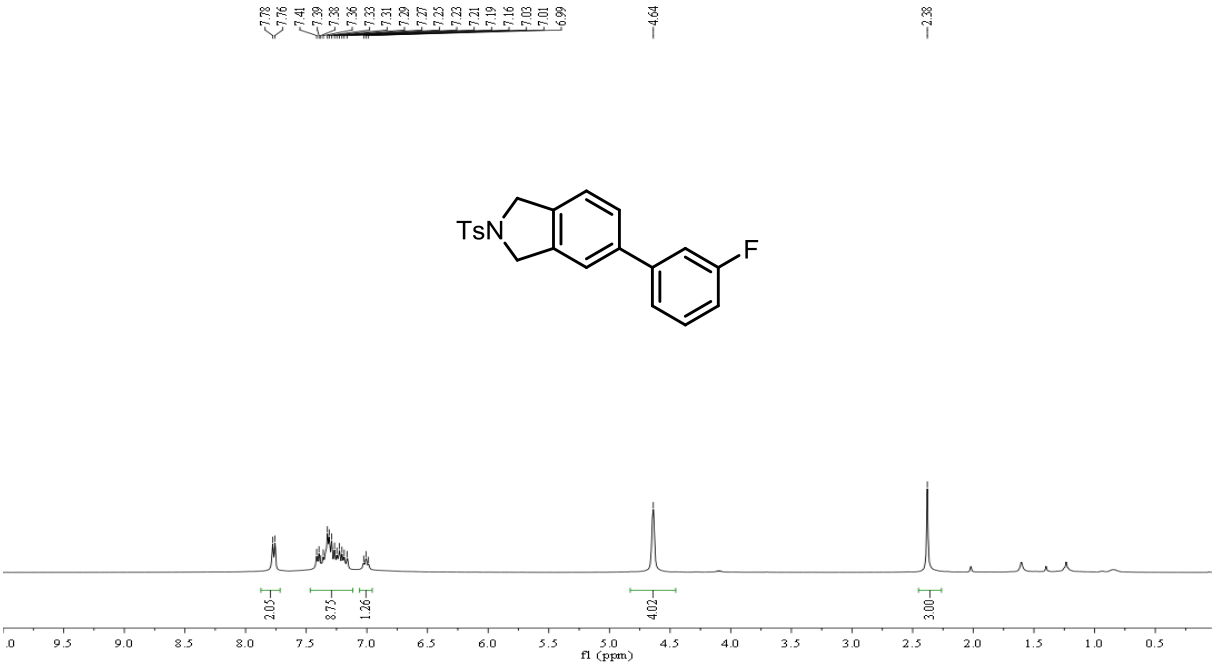

Figure S34. ^{1}H NMR (400 MHz, $CDCl_3$) of 5-(3-fluorophenyl)-2-tosylisoindoline (**3ah**).

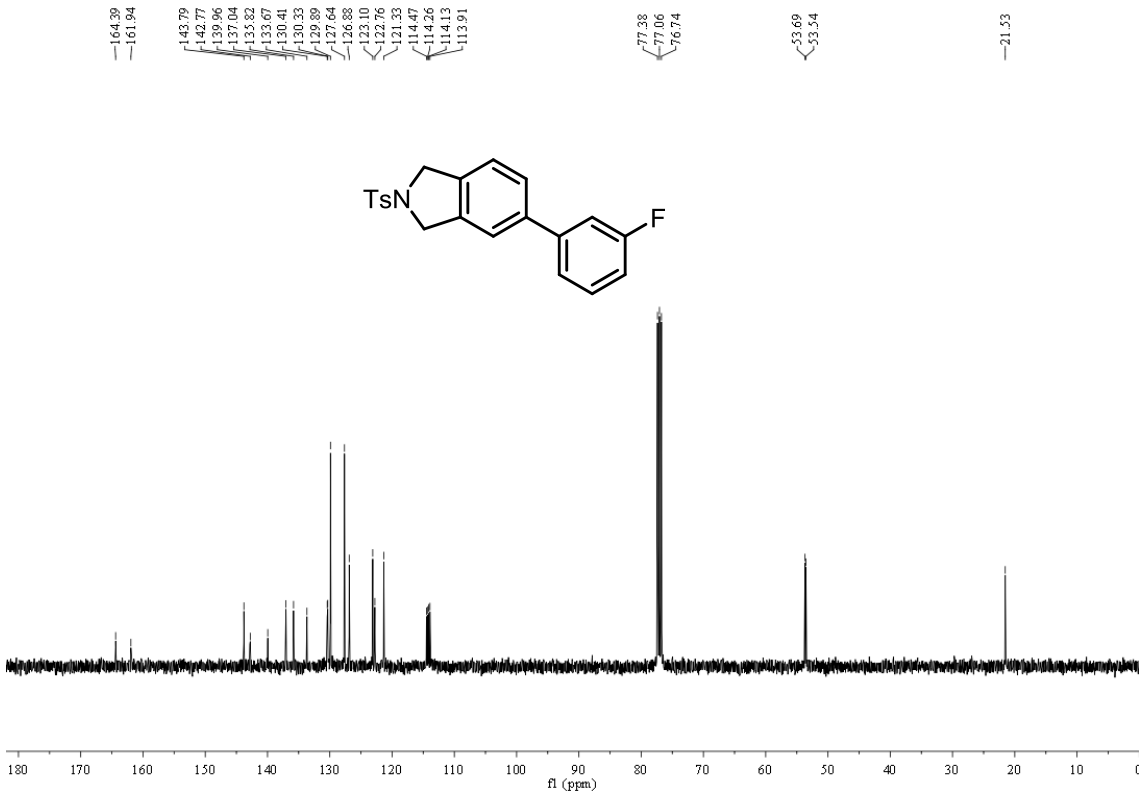

Figure S35. ^{13}C NMR (101 MHz, $CDCl_3$) of 5-(3-fluorophenyl)-2-tosylisoindoline (**3ah**).

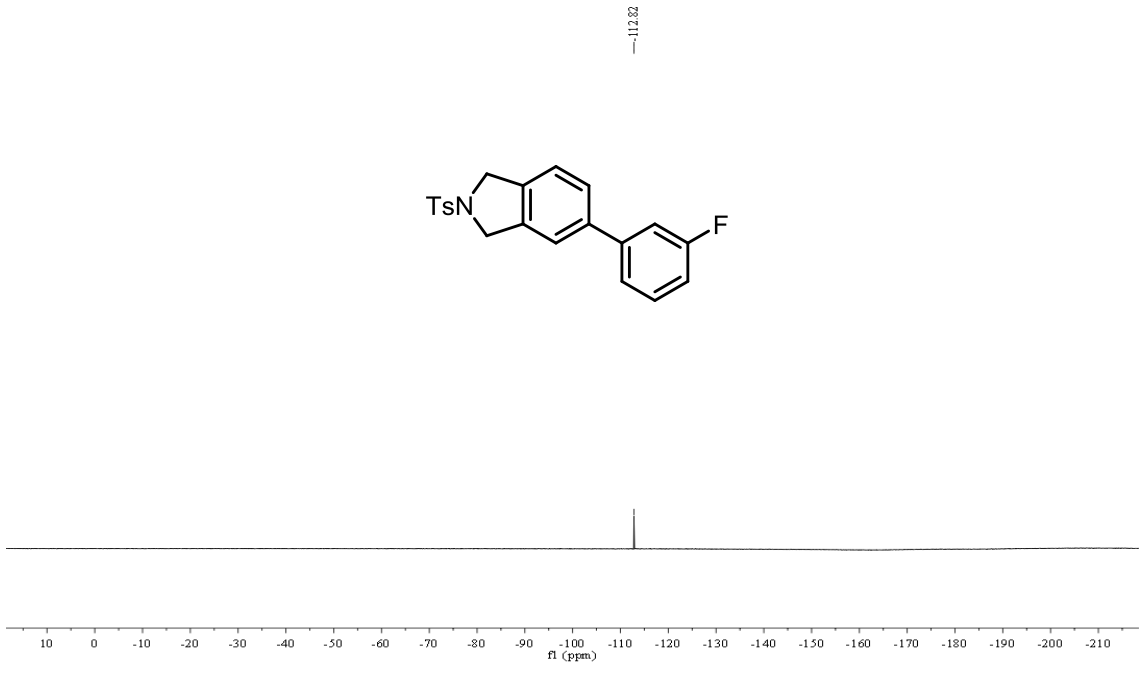

Figure S36. ^{19}F NMR (376 MHz, $CDCl_3$) of 5-(3-fluorophenyl)-2-tosylisoindoline (**3ah**).

2-((2-chlorophenyl)sulfonyl)-5-phenylisoindoline (3ba)

White solid (95% isolated yield), eluent petroleum ether/ethyl acetate = 2:1. ^{1}H NMR (400 MHz, $CDCl_3$) δ 8.16 (s, 1H), 7.74–7.19 (m, 11H), 4.87 (s, 4H). ^{13}C NMR (101 MHz, $CDCl_3$) δ 143.4, 141.4, 140.6, 136.7, 135.0, 133.7, 132.4, 132.2, 131.9, 128.9, 127.6, 127.2, 127.0, 123.0, 121.4, 100.0, 53.7, 53.5.

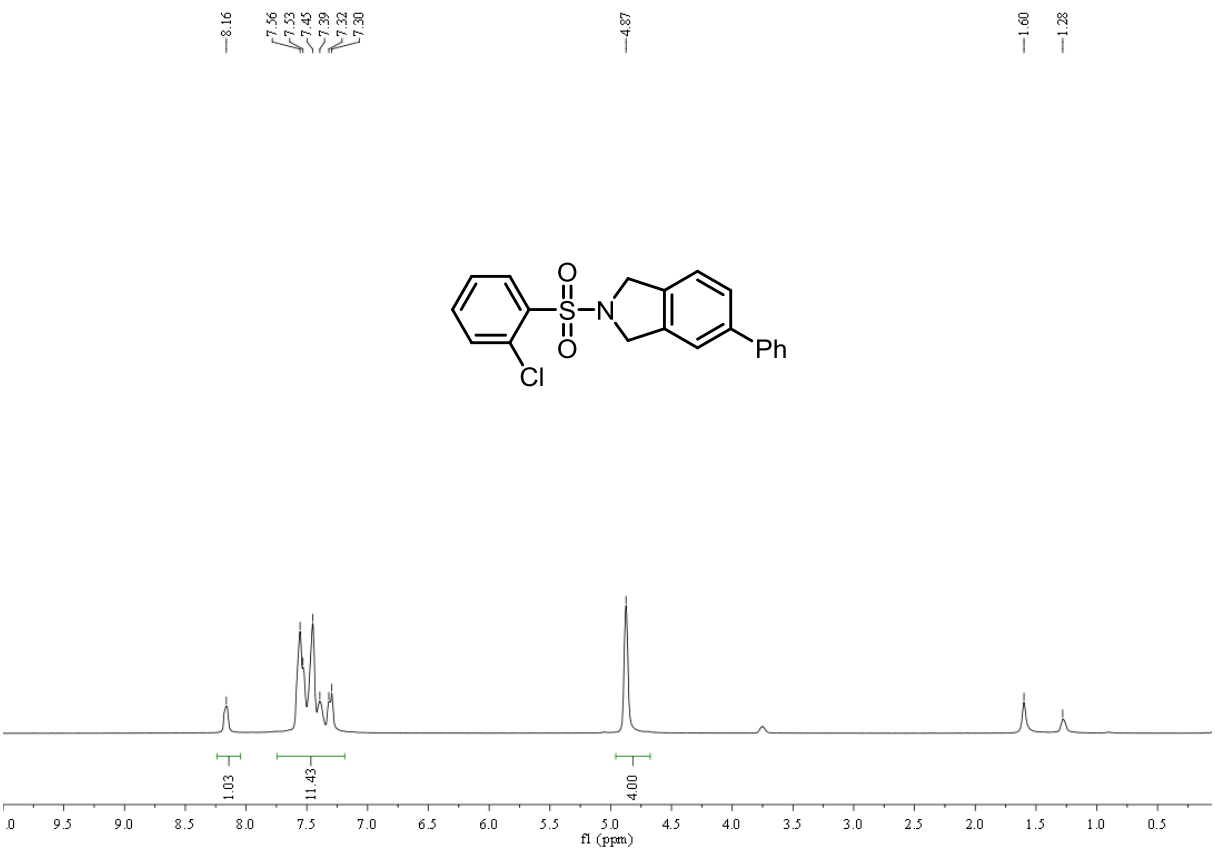

Figure S37. ^{1}H NMR (400 MHz, $CDCl_3$) of 2-((2-chlorophenyl)sulfonyl)-5-phenylisoindoline (**3ba**).

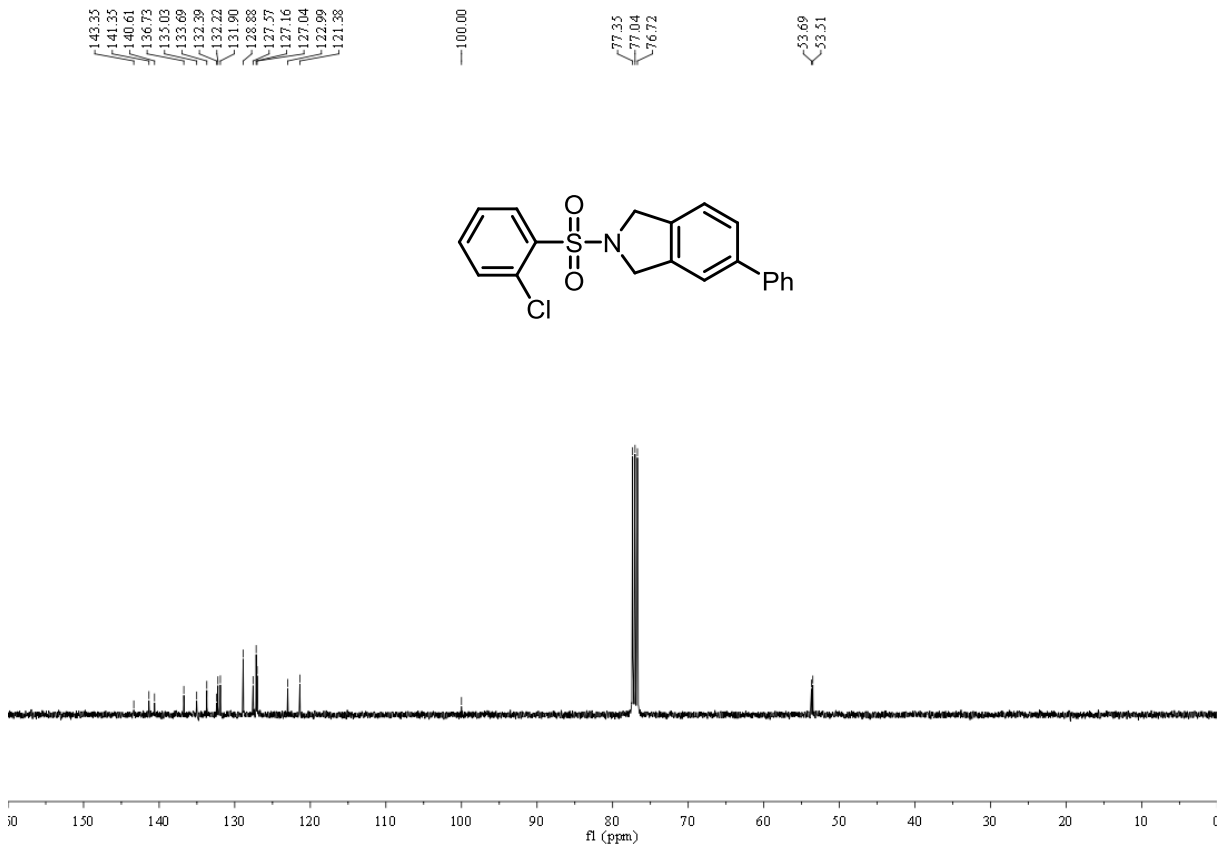

Figure S38. ^{13}C NMR (101 MHz, $CDCl_3$) of 2-((2-chlorophenyl)sulfonyl)-5-phenylisoindoline (**3ba**).

5-phenyl-2-(phenylsulfonyl)isoindoline (3ca)

White solid (92% isolated yield), eluent petroleum ether/ethyl acetate = 4:1. ^{1}H NMR (400 MHz, CDCl3) δ 7.94 (d, *J* = 7.0 Hz, 2H), 7.68–7.33 (m, 10H), 7.28 (s, 1H), 4.72 (d, *J* = 4.0 Hz, 4H). ^{13}C NMR (101 MHz, $CDCl_3$) δ 141.4, 140.5, 136.8, 135.1, 132.9, 129.3, 129.0, 128.9, 127.6, 127.6, 127.1, 127.0, 123.0, 121.4, 53.8, 53.6. HRMS calculated for $C_{20}H_{17}NO_2S$ $[M+H]^+$ 336.1058, found 336.1060.

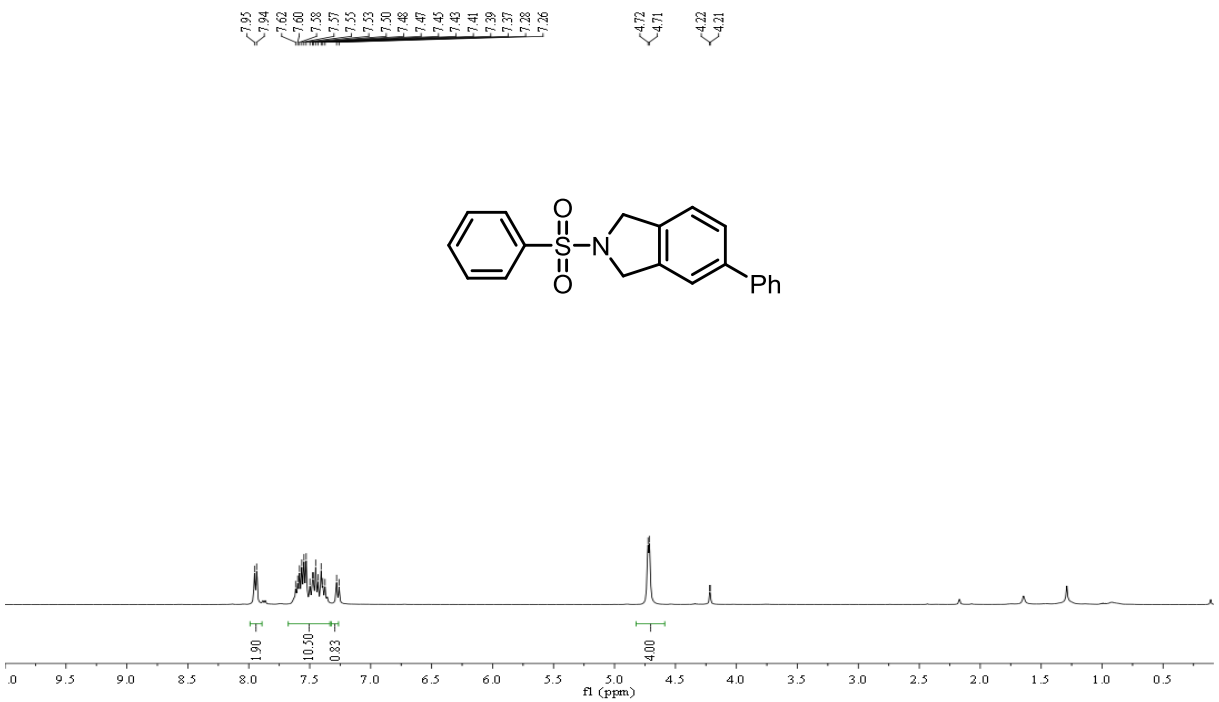

Figure S39. ^{1}H NMR (400 MHz, $CDCl_3$) of 5-phenyl-2-(phenylsulfonyl)isoindoline (**3ca**).

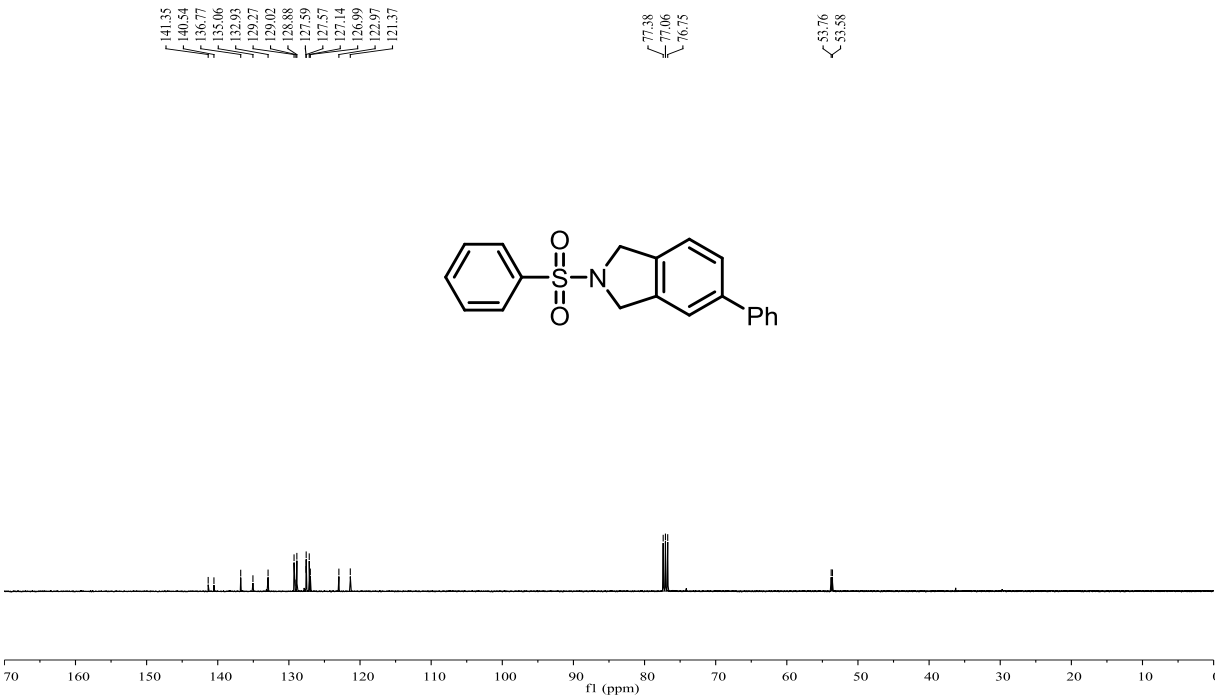

Figure S40. ^{13}C NMR (101 MHz, $CDCl_3$) of 5-phenyl-2-(phenylsulfonyl)isoindoline (**3ca**).

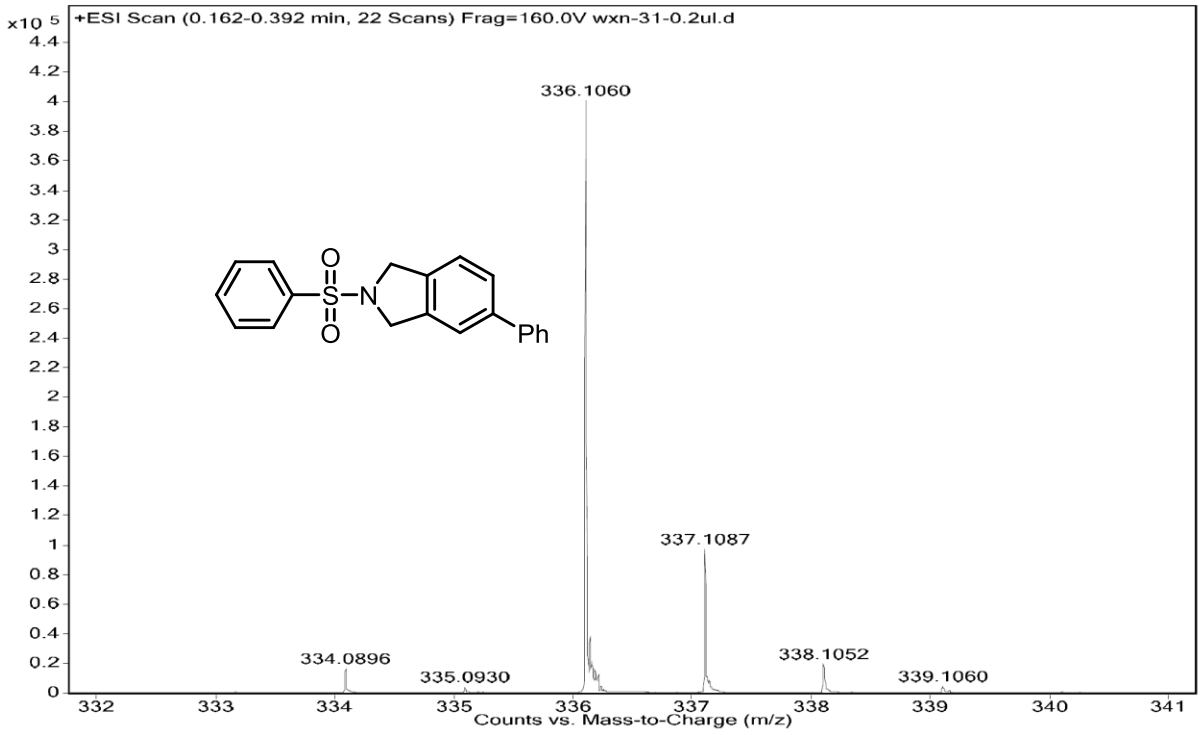

Figure S41. HRMS spectra of 5-phenyl-2-(phenylsulfonyl)isoindoline (**3ca**).

2-((2-fluorophenyl)sulfonyl)-5-phenylisoindoline (3da)

White solid (93% isolated yield), eluent petroleum ether/ethyl acetate = 2:1. ^{1}H NMR (400 MHz, $CDCl_3$) δ 8.01 (t, *J* = 7.3 Hz, 1H), 7.65–7.14 (m, 11H), 4.83 (d, *J* = 4.5 Hz, 4H). ^{13}C NMR (101 MHz, $CDCl_3$) δ 159.0 (d, *J* = 255.3 Hz), 141.4, 140.6, 136.8, 135.1 (d, *J* = 3.4 Hz), 131.4, 128.9, 127.6, 127.2, 127.0, 126.2, 126.0, 124.4 (d, *J* = 3.7 Hz) 123.0, 121.4, 117.4 (d, *J* = 22.1 Hz), 53.5 (d, *J* = 3.1 Hz), 53.3 (d, *J* = 3.1 Hz). ^{19}F NMR (376 MHz, $CDCl_3$) δ –107.18. HRMS calculated for $C_{20}H_{16}FNO_2S$ $[M+H]^+$ 354.0964, found 354.0964.

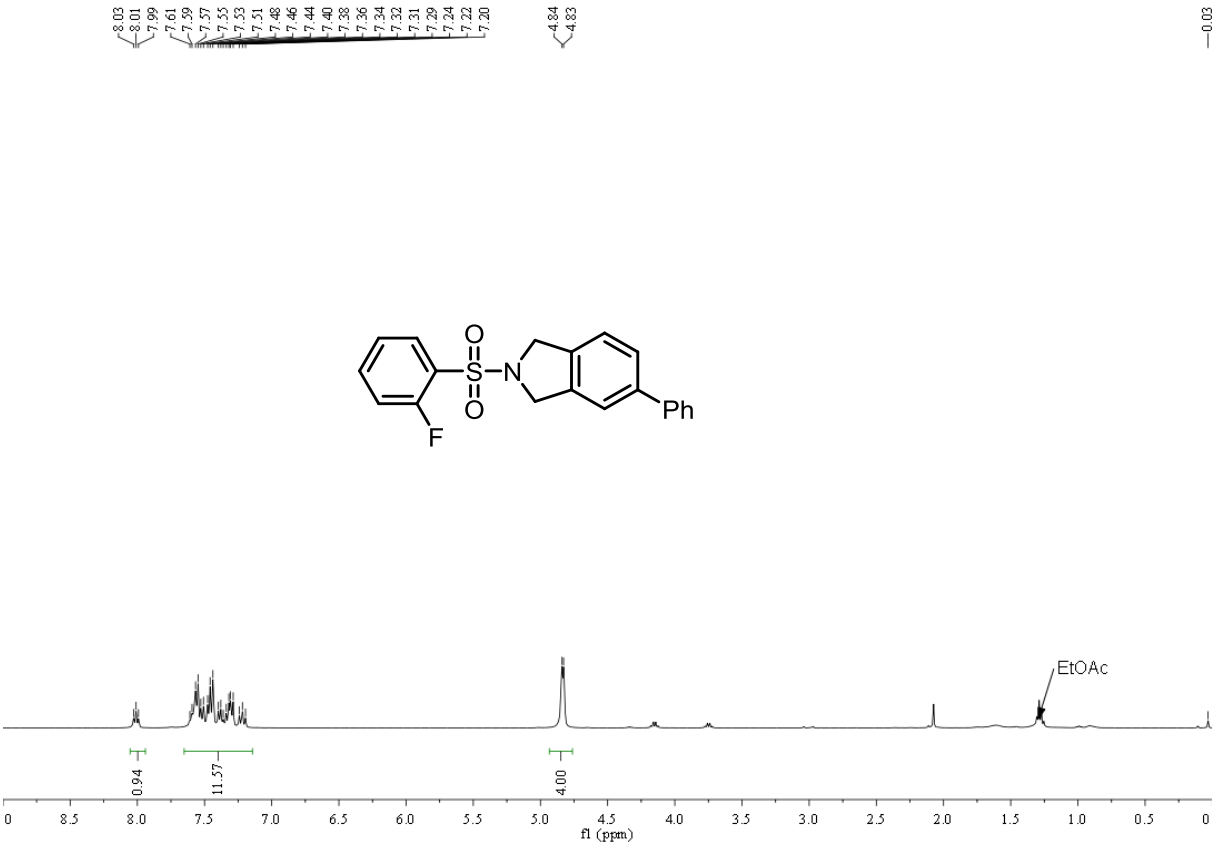

Figure S42. ^{1}H NMR (400 MHz, $CDCl_3$) of 2-benzyl-5-phenylisoindoline (**3da**).

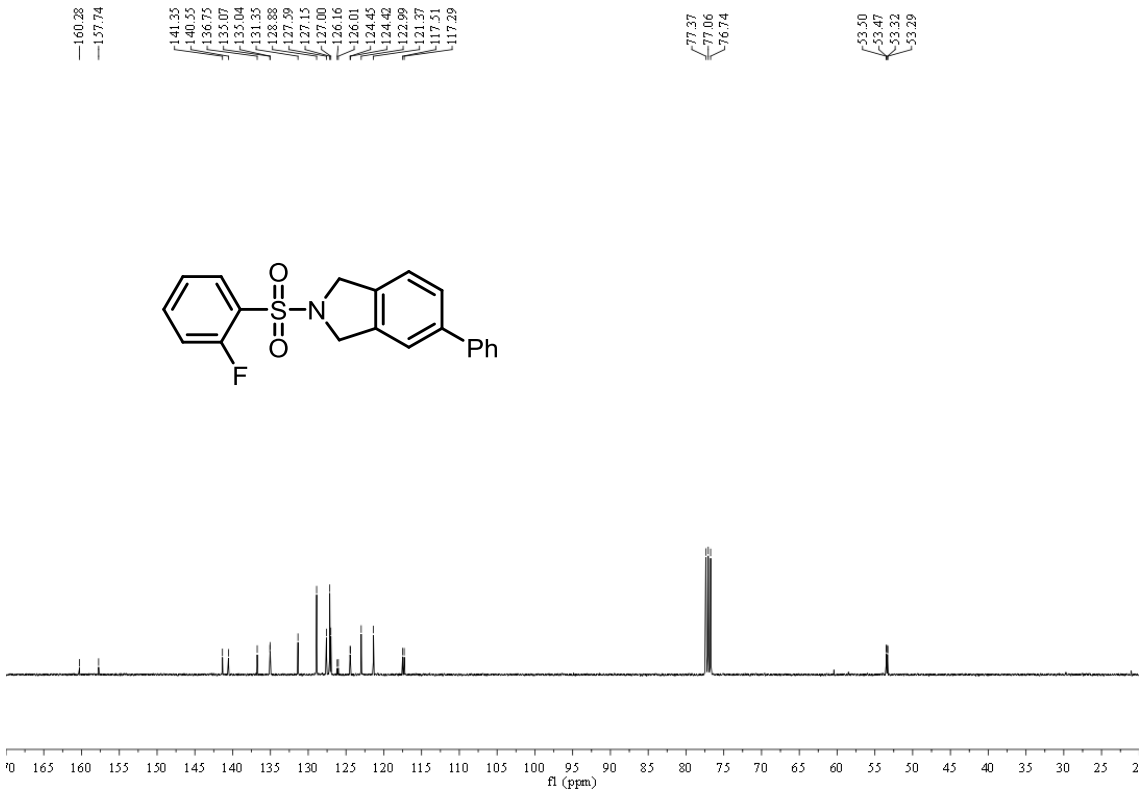

Figure S43. ^{13}C NMR (101 MHz, $CDCl_3$) of 2-benzyl-5-phenylisoindoline (**3da**).

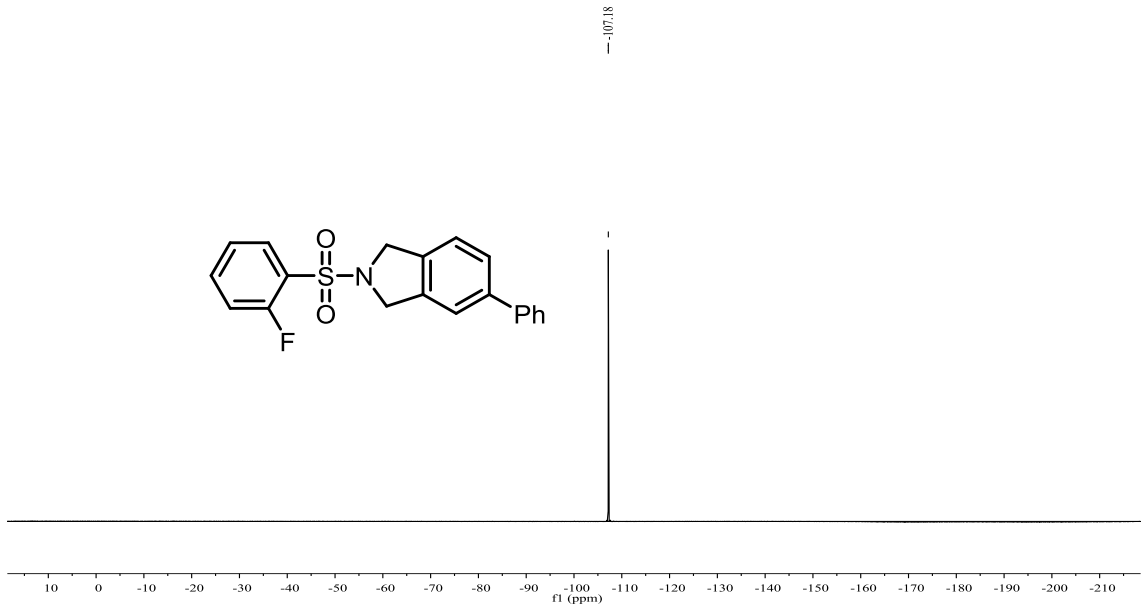

Figure S44. ^{19}F NMR (376 MHz, $CDCl_3$) of 2-benzyl-5-phenylisoindoline (**3da**).

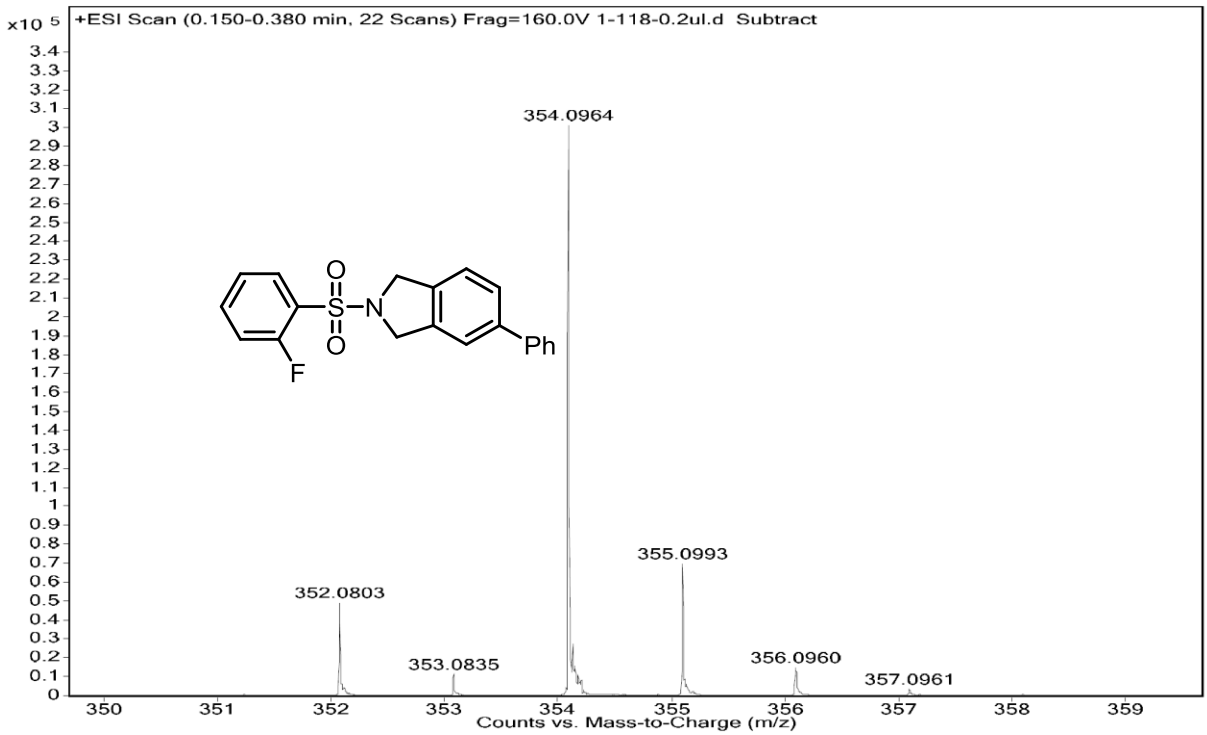

Figure S45. HRMS spectra of 2-benzyl-5-phenylisoindoline (**3da**).

phenyl(5-phenylisoindolin-2-yl)methanone (3ea)

White solid (86% isolated yield), eluent petroleum ether/ethyl acetate = 4:1. ^{1}H NMR (600 MHz, $CDCl_3$) δ 7.65–7.31 (m, 13H), 5.07 (d, *J* = 10.4 Hz, 2H), 4.82 (d, *J* = 10.1 Hz, 2H). ^{13}C NMR (151 MHz, $CDCl_3$) δ 170.5, 141.2 (d, *J* = 45.2 Hz), 140.7 (d, *J* = 4.5 Hz), 136.3 (dd, *J* = 252.8, 26.3 Hz), 135.4, 130.1, 128.9, 128.6, 127.6, 127.5, 127.2 (d, *J* = 10.6 Hz), 126.9, 126.8, 122.3 (dd, *J* = 247.3, 82.2 Hz), 55.0 (d, *J* = 27.8 Hz), 52.4 (d, *J* = 30.2 Hz).

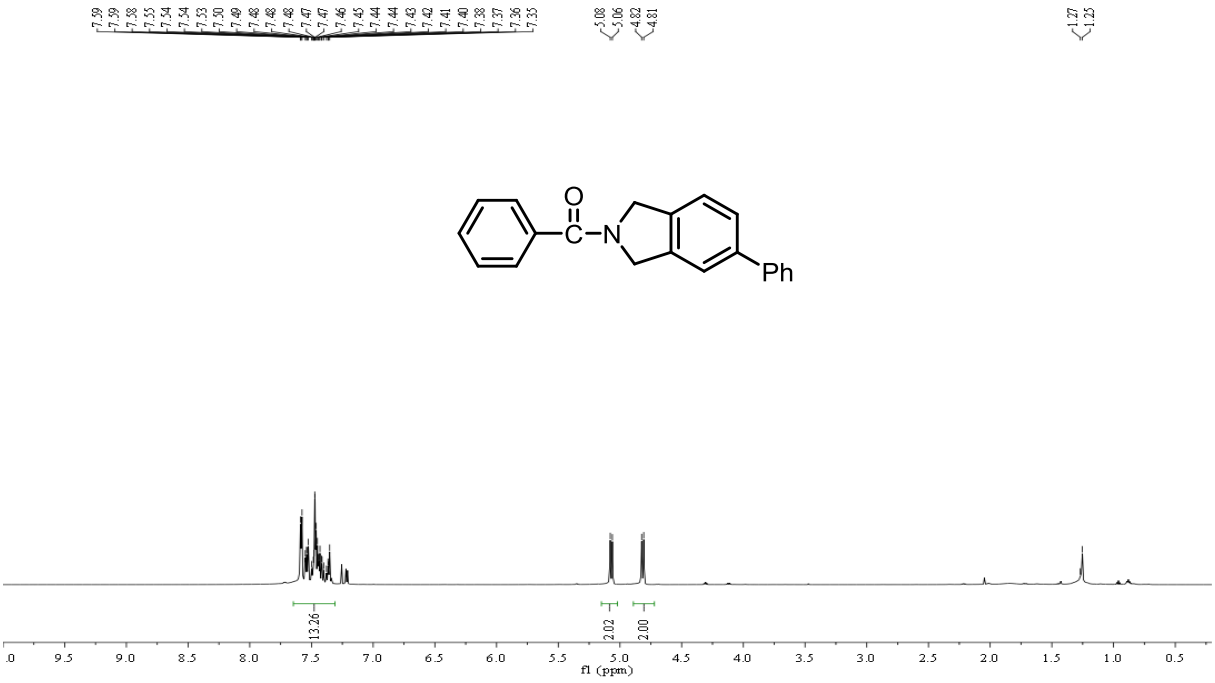

Figure S46. ^{1}H NMR (600 MHz, $CDCl_3$) of phenyl(5-phenylisoindolin-2-yl)methanone (**3ea**).

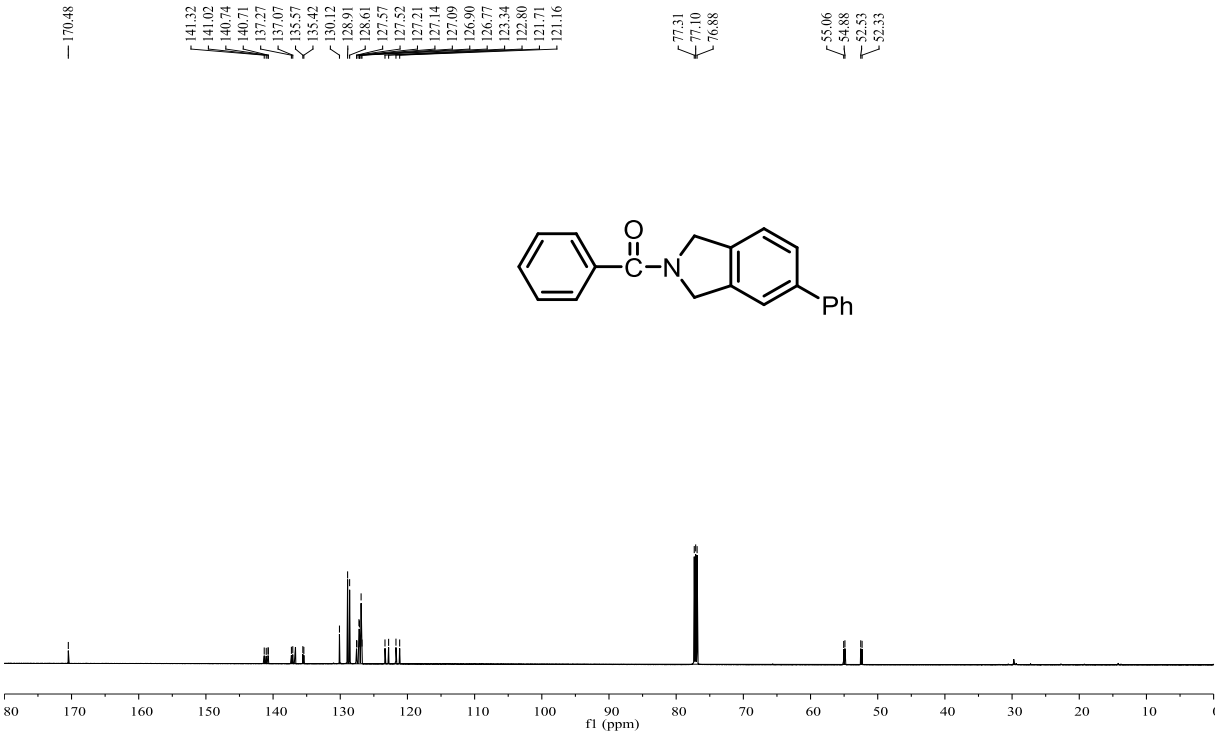

Figure S47. ^{13}C NMR (151 MHz, $CDCl_3$) of phenyl(5-phenylisoindolin-2-yl)methanone (**3ea**).

2-benzyl-5-phenylisoindoline (3fa)

White solid (84% isolated yield), eluent petroleum ether/ethyl acetate = 10:1. ^{1}H NMR (400 MHz, $CDCl_3$) δ 7.55 (d, *J* = 7.5 Hz, 2H), 7.35 (m, 11H), 4.08–3.87 (m, 6H). ^{13}C NMR (101 MHz, $CDCl_3$) δ 141.4, 140.8, 140.3, 139.2, 138.8, 128.9, 128.7, 128.5, 127.3, 127.2, 127.1, 126.0, 122.7, 121.2, 60.3, 58.9, 58.7. HRMS calculated for $C_{21}H_{19}N$ $[M+H]^+$ 286.1595, found 286.1594.

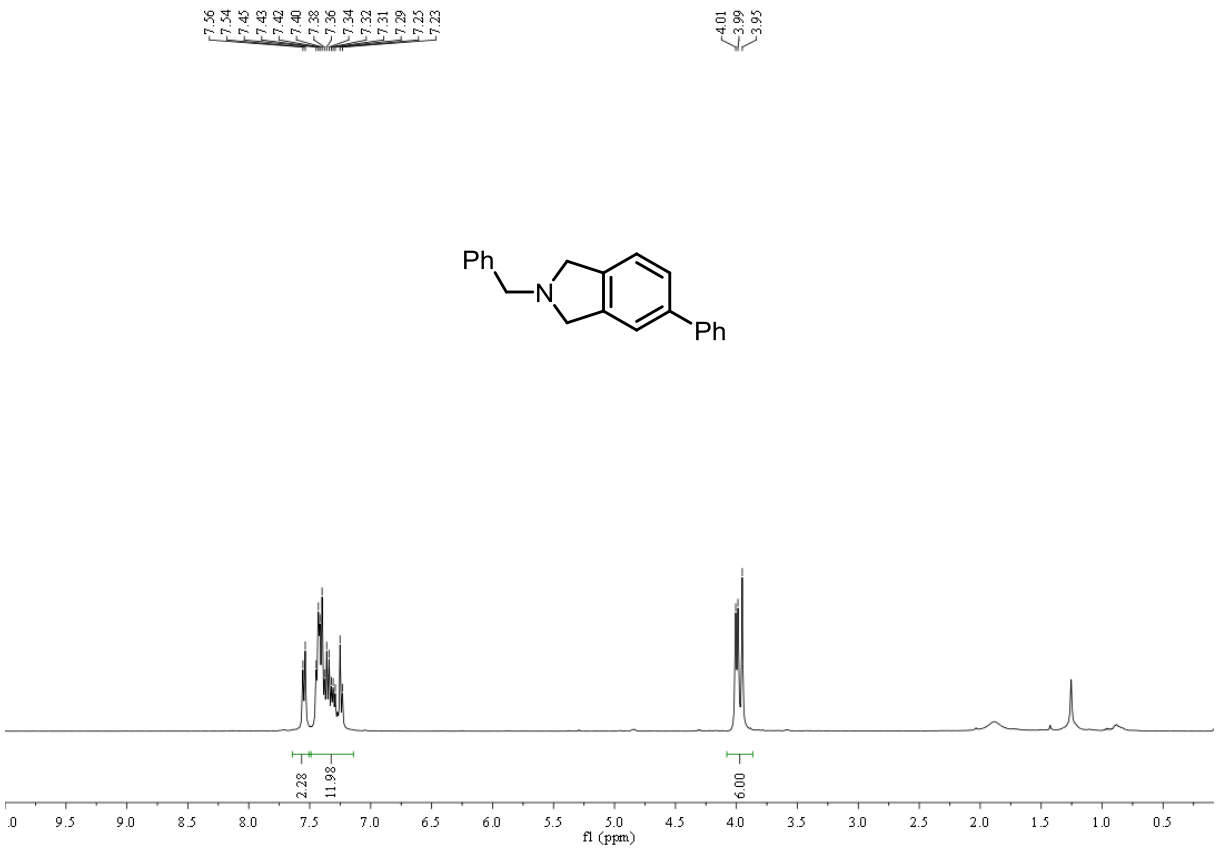

Figure S48. ^{1}H NMR (400 MHz, $CDCl_3$) of 2-benzyl-5-phenylisoindoline (**3fa**).

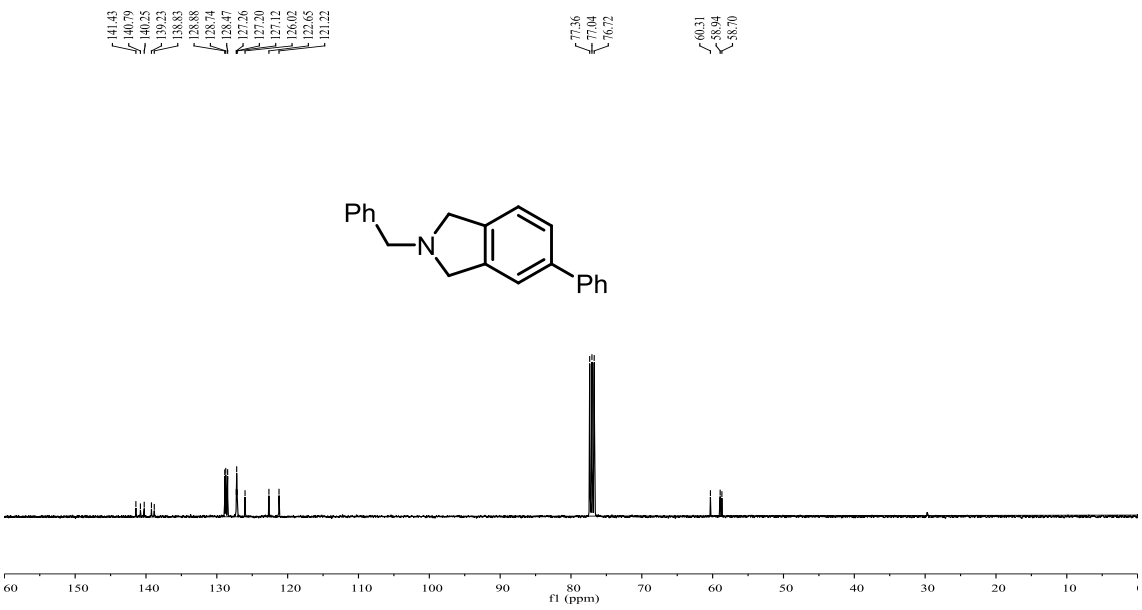

Figure S49. ^{13}C NMR (101 MHz, $CDCl_3$) of 2-benzyl-5-phenylisoindoline (**3fa**).

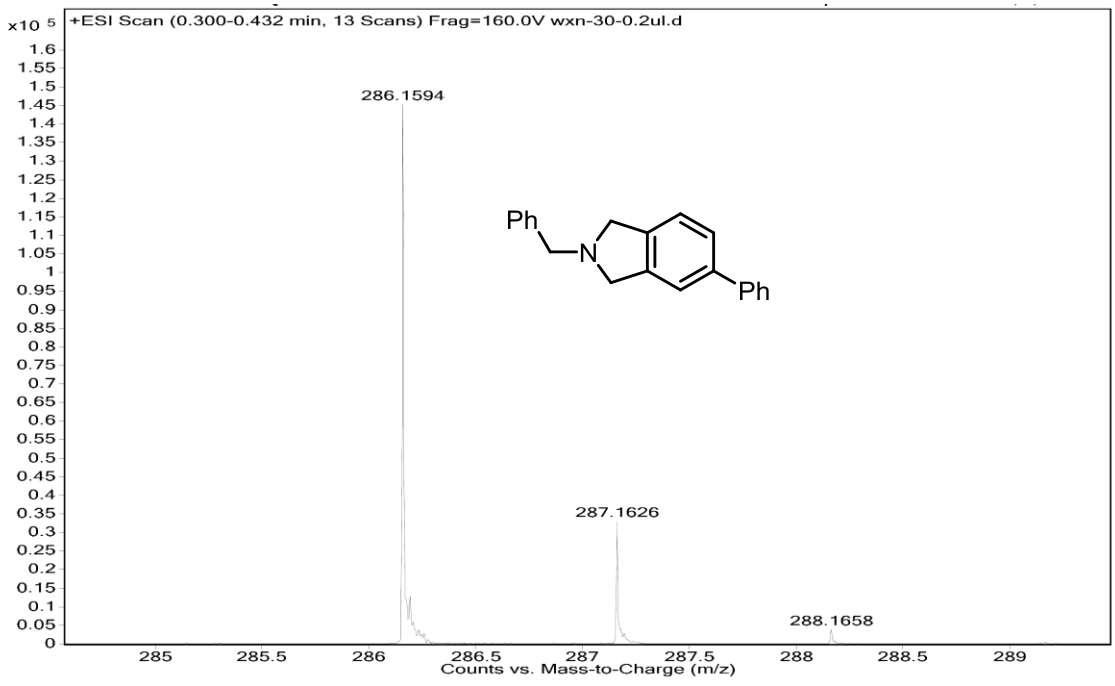

Figure S50. HRMS spectra of 2-benzyl-5-phenylisoindoline (**3fa**).

2-(methylsulfonyl)-5-phenylisoindoline (3ga)

White solid (86% isolated yield), eluent petroleum ether/ethyl acetate = 10:1. ^{1}H NMR (400 MHz, $CDCl_3$) δ 7.58 (t, *J* = 8.7 Hz, 3H), 7.52–7.44 (m, 3H), 7.38 (m, 2H), 4.78 (d, *J* = 3.1 Hz, 4H), 2.93 (s, 3H). ^{13}C NMR (101 MHz, $CDCl_3$) δ 141.5, 140.5, 136.9, 135.1, 128.9, 127.7, 127.2, 124.2, 123.1, 121.5, 53.8, 53.6, 35.0. HRMS calculated for $C_{15}H_{15}NO_2S$ $[M+H]^+$ 274.0899, found 274.0902.

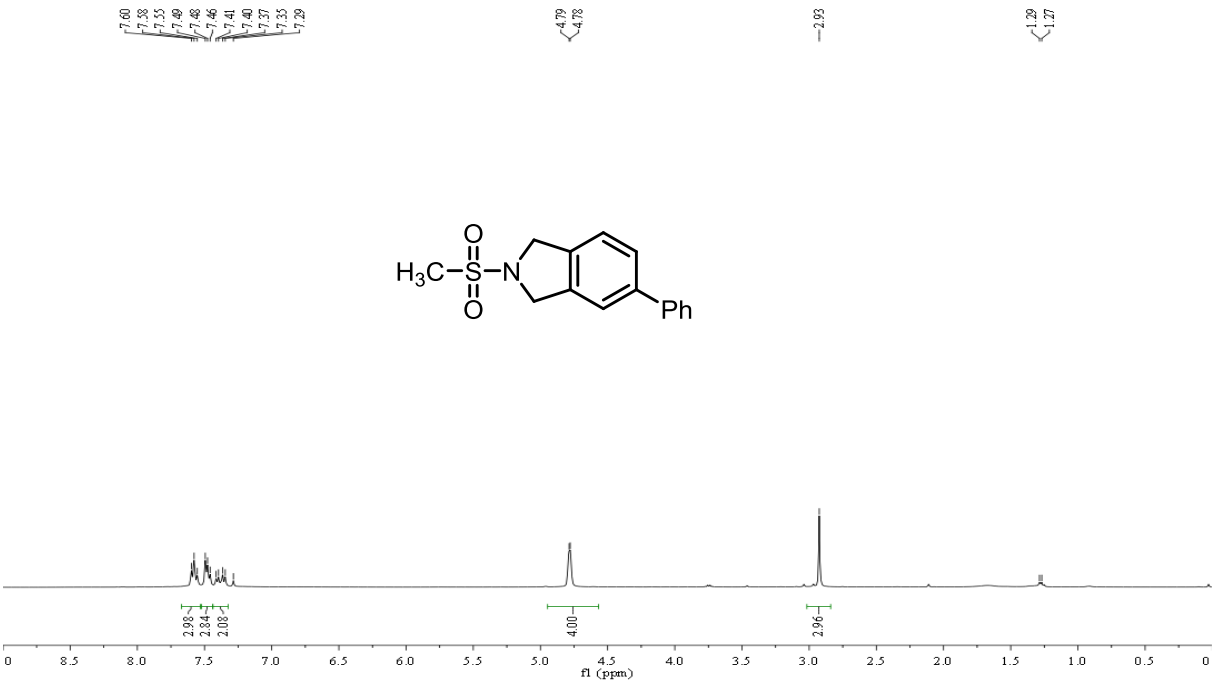

Figure S51. ^{1}H NMR (400 MHz, $CDCl_3$) of 2-(methylsulfonyl)-5-phenylisoindoline (**3ga**).

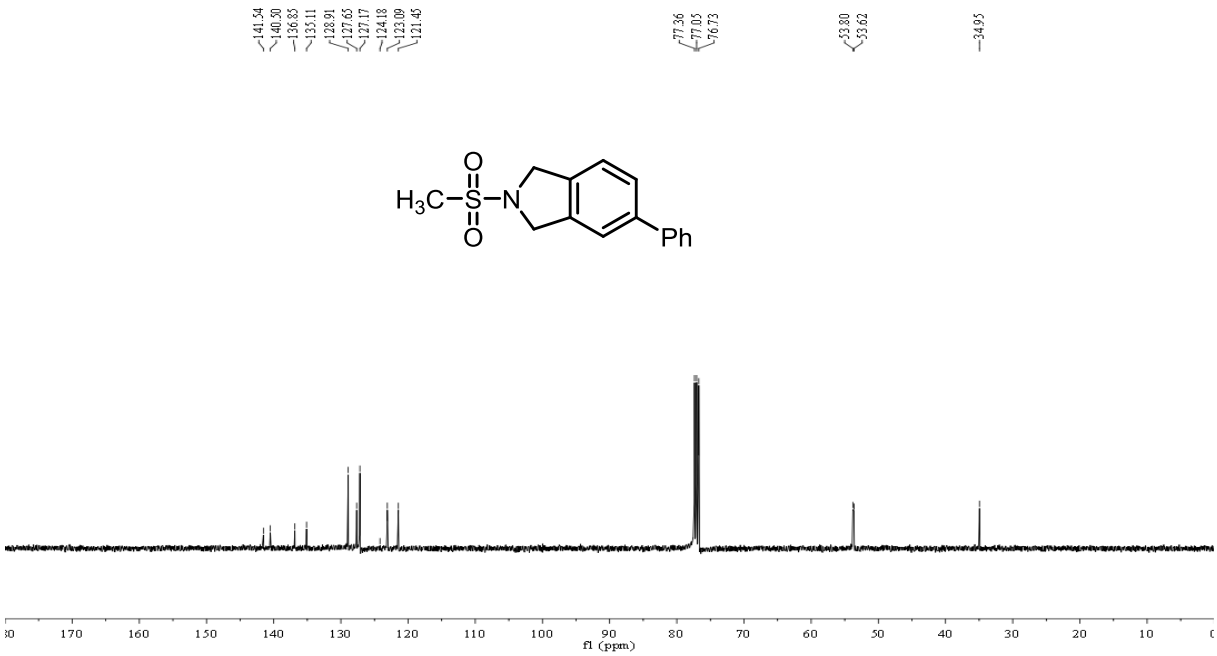

Figure S52. ^{13}C NMR (101 MHz, $CDCl_3$) of 2-(methylsulfonyl)-5-phenylisoindoline (**3ga**).

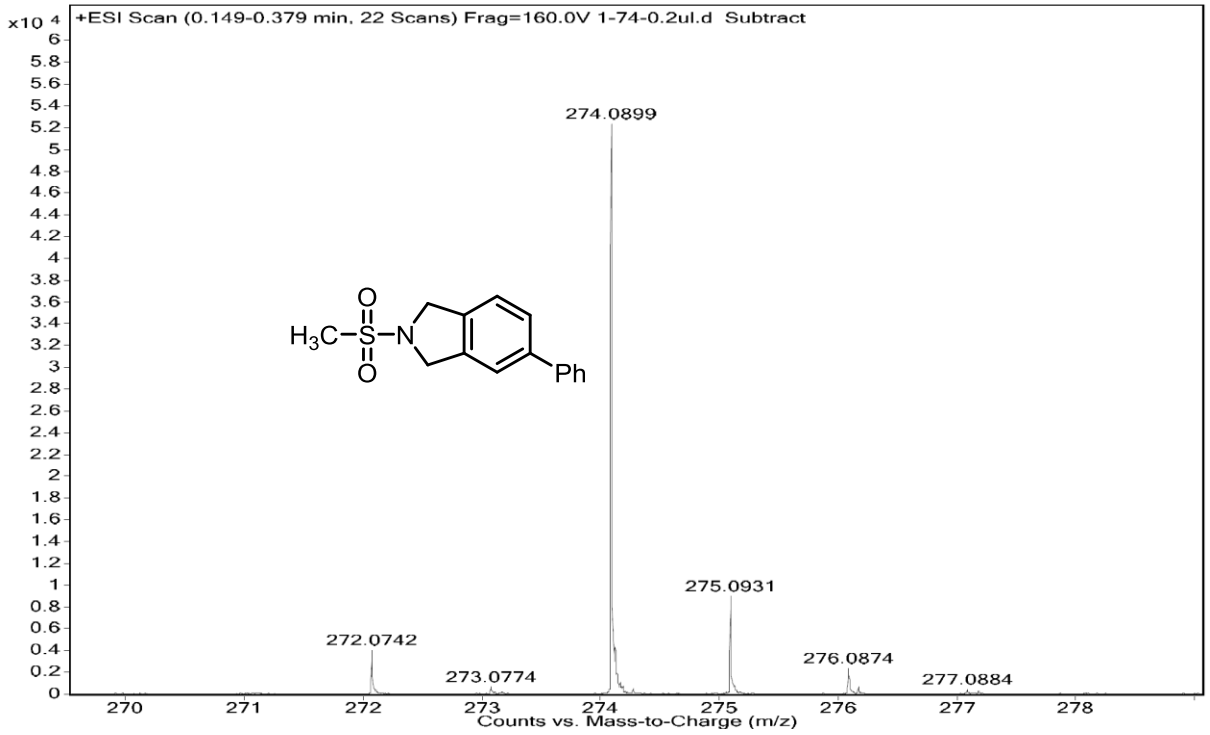

Figure S53. HRMS spectra of 2-(methylsulfonyl)-5-phenylisoindoline (**3ga**).

Dimethyl 5-phenyl-1,3-dihydro-2H-indene-2,2-dicarboxylate (3ia)

White solid (87% isolated yield), eluent petroleum ether/ethyl acetate = 10:1. ^{1}H NMR (600 MHz, $CDCl_3$) δ = 7.57–7.54 (m, 2H), 7.45–7.39 (m, 4H), 7.34 (d, *J* = 7.3, 1H), 7.28–7.26 (m, 1H), 3.77 (s, 6H), 3.66 (s, 2H), 3.64 (s, 2H). ^{13}C NMR (151 MHz, $CDCl_3$) δ = 171.1, 140.2, 139.5, 139.4, 138.0, 127.7, 126.1, 126.1, 125.2, 123.5, 122.0, 59.4, 52.1, 39.5, 39.3.

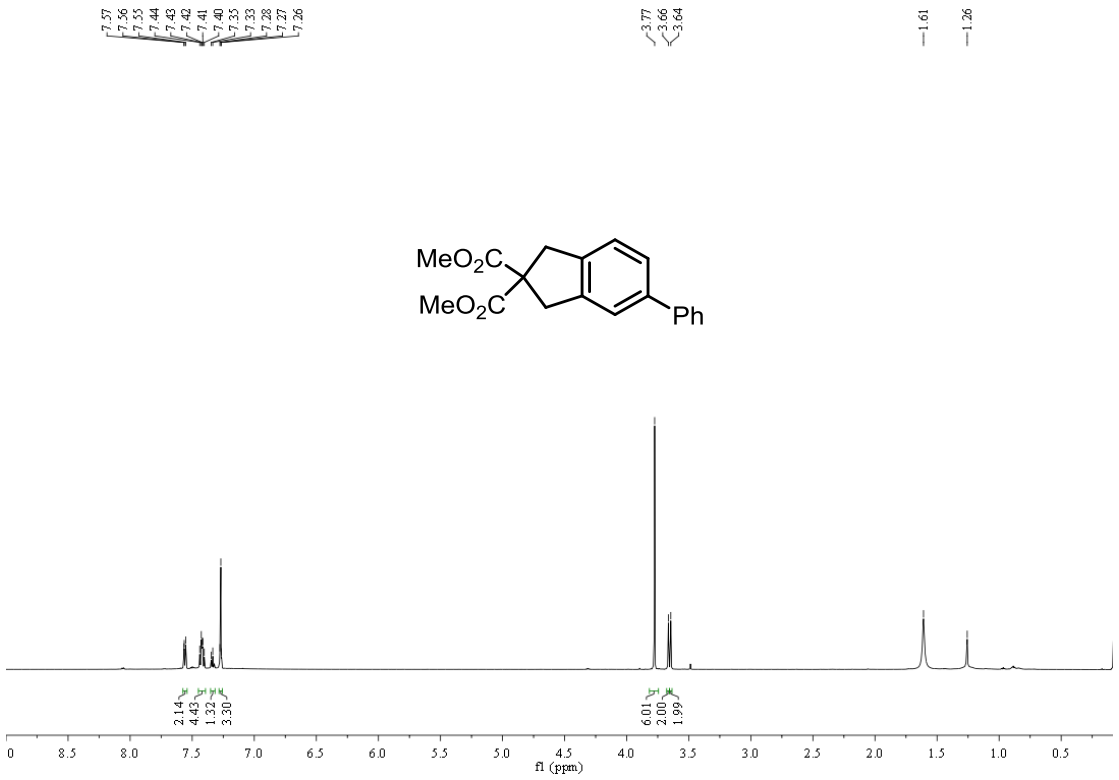

Figure S54. ^{1}H NMR (600 MHz, $CDCl_3$) of dimethyl 5-phenyl-1,3-dihydro-2H-indene-2,2-dicarboxylate (**3ia**).

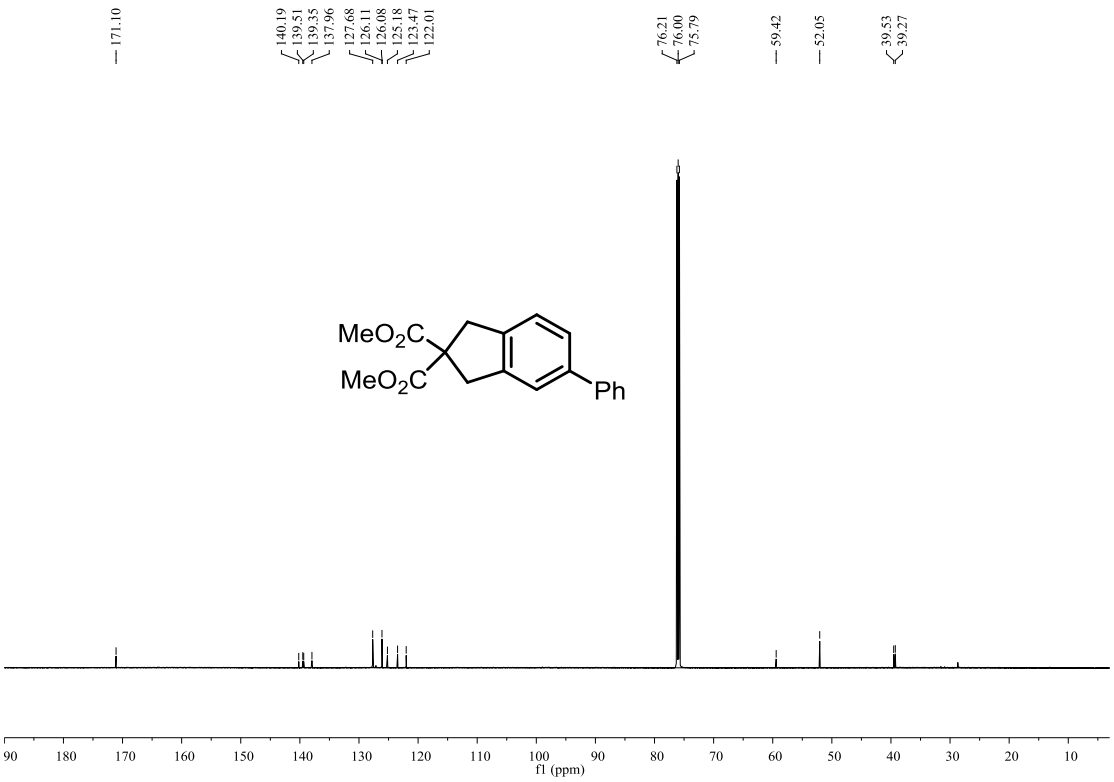

Figure S55. ^{13}C NMR (151 MHz, $CDCl_3$) of dimethyl 5-phenyl-1,3-dihydro-2H-indene-2,2-dicarboxylate (**3ia**).

5-phenyl-1,3-dihydroisobenzofuran (3ja)

White solid (84% isolated yield), eluent petroleum ether/ethyl acetate = 10:1. ^{1}H NMR (400 MHz, $CDCl_3$) δ 7.62 (d, *J* = 7.4 Hz, 2H), 7.56–7.45 (m, 4H), 7.37 (m, 2H), 5.21 (s, 4H). ^{13}C NMR (101 MHz, $CDCl_3$) δ 141.1, 140.8, 140.0, 138.3, 128.8, 127.4, 127.2, 126.6, 121.3, 119.7, 73.6, 73.5.

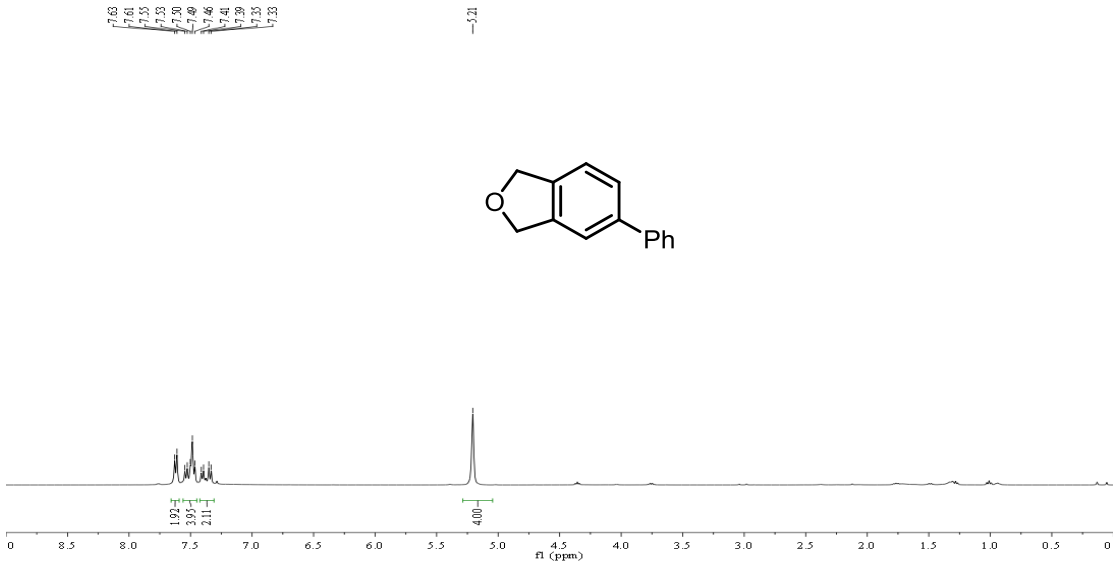

Figure S56. ^{1}H NMR (400 MHz, $CDCl_3$) of 5-phenyl-1,3-dihydroisobenzofuran (**3ja**).

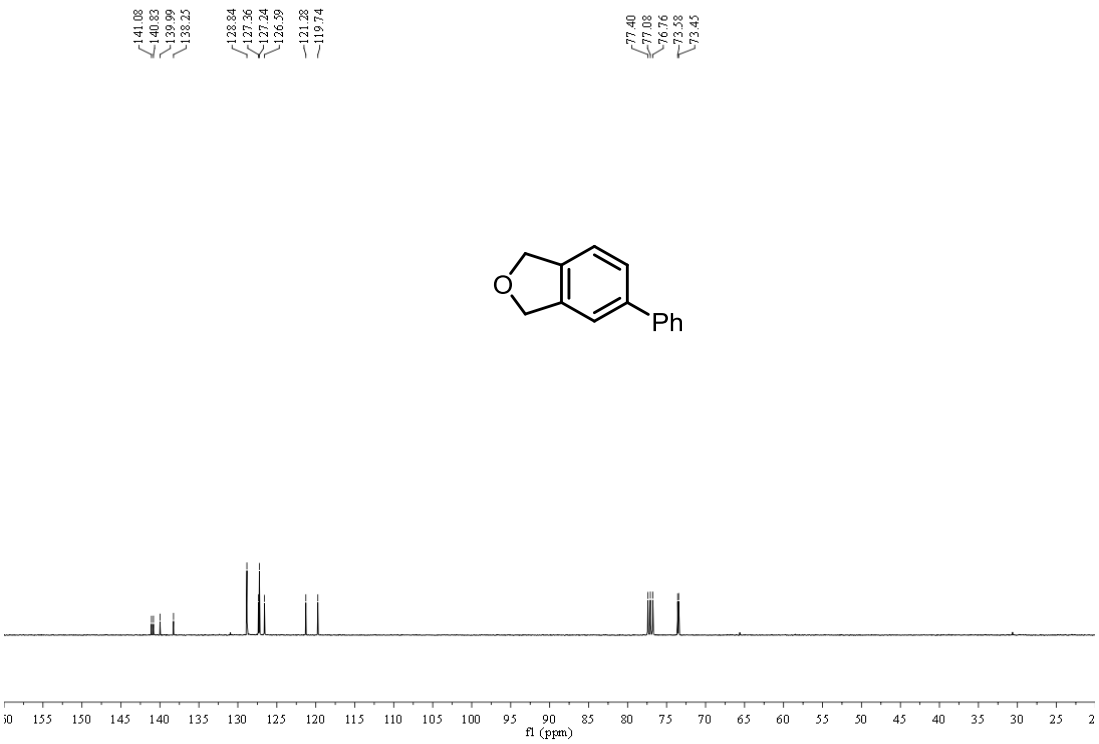

Figure S57. ^{13}C NMR (101 MHz, $CDCl_3$) of 5-phenyl-1,3-dihydroisobenzofuran (**3ja**).

References

(S1) Naik, A.; Marchand-Brynaert, J.; Garcia, Y. *Synthesis* **2008**, 149–154.

(S2) Llerena, D.; Buisine, O.; Aubert, C.; Malacria, M. *Tetrahedron* **1998**, *54*, 9373–9392.

(S3) Sperger, C.; Strand, L. H. S.; Fiksdahl, A. *Tetrahedron* **2010**, *66*, 7749–7754.

(S4) Tanaka, K.; Suzuki, N.; Nishida, G. *Eur. J. Org. Chem.* **2006**, 3917–3922.

(S5) Yamamoto, Y.; Kinpara, K.; Nishiyama, H.; Itoh, K. *Adv. Synth. Catal.* **2005**, *347*, 1913–1916.

(S6) Yamamoto, Y.; Kinpara, K.; Ogawa, R.; Nishiyama, H.; Itoh, K. *Chem. Eur. J.* **2006**, *12*, 5618–5631.

(S7) *CrysAlis CCD and CrysAlis RED*, version 1.171.37.35, Oxford Diffraction Ltd: Yarnton, Oxfordshire, U. K., 2014.

(S8) (a) Sheldrick, G. M. *SHELXTL*, version 6.10, Bruker Analytical X-ray Systems: Madison, WI, 2001. (b) Sheldrick, G. M. *Acta Cryst.* **2008**, *A64*, 112–122.

(S9) Spek, A. L. *J. Appl. Crystallogr.* **2003**, *36*, 7–13.